THE ASTROPHYSICAL JOURNAL, 558:81–108, 2001 September 1

EMPIRICAL DIAGNOSTICS OF THE STARBURST-AGN CONNECTION

R. CID FERNANDES[1]
Department of Physics and Astronomy, Johns Hopkins University, 3400 North Charles Street, Baltimore, MD 21218; cid@pha.jhu.edu
T. HECKMAN
Department of Physics and Astronomy, Johns Hopkins University, 3400 North Charles Street, Baltimore, MD 21218; heckman@pha.jhu.edu
H. SCHMITT[2]
Space Telescope Science Institute; and National Radio Astronomy Observatory, P.O. Box O, Socorro, NM 87801; hschmitt@nrao.edu
R. M. GONZÁLEZ DELGADO
Instituto de Astrofísica de Andalucía (CSIC), Apto. 3004, 18080 Granada, Spain; rosa@iaa.es
AND
T. STORCHI-BERGMANN
Instituto de Física, Universidade Federal do Rio Grande do Sul, C.P 15001, 91501-970, Porto Alegre, RS, Brazil; thaisa@if.ufrgs.br
Received 2001 January 24; accepted 2001 May 2

ABSTRACT

We examine a representative sample of 35 Seyfert 2 nuclei. Previous work has shown that nearly half (15) of these nuclei show the direct (but difficult to detect) spectroscopic signature at optical/near-UV wavelengths of the hot massive stars that power circumnuclear starbursts. In the present paper we examine a variety of more easily measured quantities for this sample, such as the equivalent widths of strong absorption features, continuum colors, emission line equivalent widths, emission line ratios and profiles, far-IR luminosities, and near-UV surface brightness. We compare the composite starburst + Seyfert 2 nuclei to "pure" Seyfert 2 nuclei, Starburst galaxies, and normal galactic nuclei. Our goals are to verify whether the easily measured properties of the composite nuclei are consistent with the expected impact of a starburst and to investigate alternative less demanding methods to infer the presence of starbursts in Seyfert 2 nuclei, applicable to larger or more distant samples. We show that starbursts do indeed leave clear and easily quantifiable imprints on the near-UV to optical continuum and emission line properties of Seyfert 2's. Composite starburst + Seyfert 2 systems can be recognized by: (1) a strong "featureless continuum" (FC), which dilutes the Ca II K line from old stars in the host's bulge to an equivalent width $W_K < 10$ Å; (2) emission lines whose equivalent widths are intermediate between starburst galaxies and "pure" Seyfert 2's; (3) relatively low excitation line ratios, which indicate that part of the gas ionization in these Seyfert 2's (typically $\sim 50\%$ of Hβ) is due to photoionization by OB stars; (4) large far-IR luminosities ($\gtrsim 10^{10}\ L_\odot$); (5) high near-UV surface brightness ($\sim 10^3\ L_\odot\ \mathrm{pc}^{-2}$). These characteristics are all consistent with the expected impact of circumnuclear starbursts on the observed properties of Seyfert 2's. Furthermore, they offer alternative empirical diagnostics of the presence of circumnuclear starbursts from a few easily measured quantities.

Subject headings: galaxies: active — galaxies: nuclei — galaxies: Seyfert
On-line material: machine-readable table

1. INTRODUCTION

The role of starbursts in active galactic nuclei (AGNs) is an issue which permeates the history of AGN literature. Theoretical scenarios for a "starburst-AGN connection" vary from those in which starbursts are a key piece of the AGN machinery, either through symbiotic or evolutionary processes (e.g., Perry & Dyson 1985; Sanders et al. 1988; Norman & Scoville 1988; Rees 1989; Daly 1990; Terlevich et al. 1992; Williams, Baker, & Perry 1999), to those in which these are fundamentally decoupled phenomena, but which are likely to coexist merely because both are triggered by and live on gas fueling (e.g., Byrd et al. 1986; Byrd, Sundelius, & Valtonen 1987; Lin, Pringle, & Rees 1988; Heller & Shlosman 1994; Hernquist & Mihos 1995; Mihos & Hernquist 1996). Given the enormous breadth of possibilities in between these extremes, it is likely that progress in understanding this connection will be driven more by input from observations than from theoretical considerations.

Observational work during the past decade has indeed substantially advanced our ability to recognize starbursts in the complex inner environment of AGNs. Optical and UV studies of Seyfert 2 galaxies have been particularly enlightening in this respect. In a series of papers (Heckman et al. 1997; Cid Fernandes, Storchi-Bergmann, & Schmitt 1998; González Delgado et al. 1998; Storchi-Bergmann, Cid Fernandes, & Schmitt 1998; Schmitt, Storchi-Bergmann, & Cid Fernandes 1999; Storchi-Bergmann et al. 2000; González Delgado, Heckman, & Leitherer 2001) we have detected unambiguous signatures of young massive stars within ~ 300 pc of the nucleus in 30% to 50% of Seyfert 2's by means of high-quality optical and, whenever possible, UV spectroscopy. This result fits well with the near-IR

[1] Gemini Fellow. On leave of absence from Depto. de Física-CFM, UFSC, Florianópolis, SC, Brazil.
[2] Jansky Fellow.

studies of Oliva et al. (1995, 1999), which find a comparable incidence of starbursts in Seyfert 2's through measurements of the stellar mass-to-light ratio. The starbursts in these composite starburst + AGN systems can make a significant contribution to the total luminosity output. In fact, studies specifically aimed at candidate composite galaxies, as selected by emission line ratios intermediate between H II regions and AGNs on classical diagnostic diagrams, demonstrate that their far-IR and radio properties are dominated by star-forming activity at the 90% level (Hill et al. 2001, 1999). Even the presence of compact radio cores, a more classical indicator of AGN activity (Condon et al. 1991; Sramek & Weedman 1986; Norris et al. 1990), can be accounted for by star formation (Hill et al. 2001; Kewley et al. 2000; Smith et al. 1998a, 1998b; Lonsdale, Smith, & Lonsdale 1993). Other recent results are covered in the review by Veilleux (2001) and the volume edited by Aretxaga, Kunth, & Mugica (2001).

Evidence is also steadily accumulating that associates AGNs with star formation on galactic scales. The ubiquity of supermassive black holes in the nuclei of normal galaxies in the local universe (Ho 1999), the proportionality between bulge and black hole masses (Magorrian et al. 1998; Gebhart et al. 2000; Ferrarese & Merrit 2000), the link between $M_{\rm black\text{-}hole}/M_{\rm bulge}$ and the age of the last major star formation episode in the spheroid (Merrifield, Forbes, & Terlevich 2000), all imply that the creation of these black holes and the ensuing QSO activity were an integral part of the formation of ellipticals and galactic bulges. This fossil evidence indirectly traces a much more active past, in which both copious star formation and nuclear activity coexisted. Since the technology to directly study this high-redshift era in detail is not available, we must guide our study of the starburst-AGN connection by data gathered on nearby objects in which traces of this connection are caught in fraganti. This means refining our knowledge of circumnuclear starbursts in Seyfert galaxies. In the optical-UV range, as hinted above, this is best accomplished studying type 2 Seyferts. Their favorable geometry, in which the blinding glare of the nucleus is blocked away by a dusty torus, facilitates the detection of features from circumnuclear starbursts, thus making them the best-suited local laboratories to study the starburst-AGN connection.

Advancing our empirical understanding of circumnuclear starbursts in Seyfert galaxies can be described as a three-stage process: (I) Identifying starbursts in these systems; (II) characterizing the properties of the starburst (age and mass, or star formation rate) and the AGN (black hole mass, accretion rate); and (III) investigating possible connections between these properties. Once we get to this third stage fundamental questions can start to be addressed. For instance: Is star formation inextricably associated with AGN activity? Are the starburst and AGN powers related, say, by a $M_{\rm starburst} \propto M_{\rm black\text{-}hole}$ proportionality between their masses? Or, analogously, is the star formation rate connected to the rate of accretion onto the nuclear supermassive black hole? Does the central engine evolve in parallel to the starburst around it? Much work remains to be done before tackling these key questions.

The work on Seyfert 2's reviewed above pertains mostly to stage I of this process, as it essentially demonstrates how certain spectral features of massive stars can be used as signposts of starburst activity. Estimates of the recent history of star formation in the circumnuclear regions were also presented, thus touching the domain of stage II. These estimates come associated with known difficulties in accurately retrieving the detailed star formation history of stellar systems (e.g., Leitherer 1999; Cid Fernandes et al. 2001; Kennicutt 1998), but they represent the current state of the art regarding the characterization of the basic starburst properties.

This paper deals mainly with stage I, that is, the identification of starbursts in Seyfert 2's, using the data sets of Cid Fernandes et al. (1998) and González Delgado et al. (2001, hereafter GD01) as a training set. This is probably the largest sample whose optical spectra have been systematically and carefully screened for starburst features, so it represents a good starting point. The analysis is geared toward verifying whether composite Seyfert 2/starburst systems, those in which stellar features produced by young populations have been directly detected, exhibit other properties which differentiate them from systems not showing signs of starburst activity ("pure" Seyfert 2's). Unlike the detailed analysis reported by the previous work on these data, we here limit ourselves to easily measurable quantities. Specifically, we will use equivalent widths of strong absorption bands and continuum colors in the near-UV, emission line equivalent widths, fluxes, and line ratios, far-IR luminosities, and near-UV surface brightness. The purpose of this analysis is twofold:

1. To verify whether the optical continuum and emission line properties of composite systems are consistent with the expected impact of starbursts upon these observables.
2. To investigate alternative ways to infer the presence of circumnuclear starbursts in Seyfert 2's that may provide more straightforward diagnostics applicable to larger and/or more distant samples.

The first of these points serves both as a consistency check and to give a sense of the role played by starbursts in the phenomenology and energetics of AGNs. The relevance of the second point is that increasing the statistics is crucial to improve upon the still sketchy overall census of circumnuclear starbursts in Seyfert 2's, to extend these studies to higher redshifts and to provide the raw material for further stage II and III studies.

In § 2 we describe the data for the Seyfert 2's and comparison samples used in this study. In § 3 we deal with the problem of estimating the "featureless continuum" (FC) strength. We apply a method based on population synthesis, but which can be parameterized in terms of a few easily measurable quantities. Essentially, we are able to estimate the FC contribution to the optical light with little more than the equivalent width of the Ca II K absorption line, a method which may be of wide applicability in Seyfert 2 studies. In § 4 we present an analysis of the emission line equivalent widths, line ratios, and profiles, and discuss how they are affected by the presence of circumnuclear starbursts. Emission line-FC correlations are also presented and discussed. In § 5 we investigate how the composite systems behave in terms of far-IR luminosity and how they fare in comparison to normal and interacting galaxies. In § 6 we compare the near-UV surface brightness of Seyfert 2's in our sample to that of normal and Starburst galaxies. In § 7 we collect the results obtained in a set of empirical criteria which may be used to diagnose the presence of circumnuclear starbursts in Seyfert 2's. We also discuss the

meaning of the composite/"pure" Seyfert 2 classification and present tentative evidence of evolutionary effects in our sample. Section 8 summarizes our conclusions.

2. THE DATABASE

In this study we merge the Seyfert 2's in the southern sample studied by Cid Fernandes et al. (1998) with those in the northern sample of GD01, totaling 35 galaxies. Details of the observations, sample selection, and previous analysis of these data can be found in the original papers and Heckman et al. (1997), González Delgado et al. (1998), Storchi-Bergmann et al. (1998), Schmitt et al. (1999), and Storchi-Bergmann et al. (2000, hereafter SB00). We concentrate our analysis on the nuclear spectra, extracted through $1\farcs2 \times 2\farcs1$ apertures for the northern sample and $2'' \times 2''$ for the southern one. At the distances of our galaxies this covers a region 60–860 pc in radius, with a median of 300 pc ($H_0 = 75$ km s^{-1} Mpc^{-1} is adopted throughout this paper). We will also focus on the near-UV to optical region of the spectrum, between 3500 and 5100 Å.

These 35 galaxies will hereafter be referred to as the "Seyfert 2 sample." They constitute a good data set to investigate the starburst-AGN connection because the above papers have scrutinized these sources in search for signs of a starburst component. Specifically, the following signatures of a starburst were examined: (1) the presence of far-UV stellar wind lines (N v λ1240, Si iv λ1397, and C iv λ1549) due to O stars; (2) high-order Balmer absorption lines of H i and He i in the near-UV; (3) the WR bump underneath He ii λ4686. The far-UV features are the cleanest signatures of recent star formation, but, unfortunately, there are only a handful of Seyfert 2's for which *HST* far-UV spectroscopy is feasible. All four galaxies in the sample for which we acquired such data (Mrk 477, NGC 5135, NGC 7130, and IC 3639) have their far-UV spectrum dominated by young stars. For the remaining galaxies, detection of a starburst component relies on either high-order Balmer lines, which originate in the photosphere of O, B, and A stars, or the WR bump, a tracer of very recent (3–6 Myr) star formation. Although more subtle than the far-UV features, these are reliable and more easily accessible indicators of the presence of a starburst. This is confirmed by the fact that either of these two features is also detected in the galaxies for which we have identified stellar wind lines in the far-UV. The least certain of these diagnostics is the WR bump, because independent evidence of the presence of WR stars is hard to obtain (GD01; Shaerer 2001). Nevertheless, this is the simplest interpretation of this feature, given the similarity to the feature sometimes seen in star-forming galaxies ("WR galaxies"), the lack of convincing alternatives, and the simultaneous detection of other starburst features in some of the sources.

The information to be used in this paper comprises fluxes and equivalent widths (W) of the [O ii] $\lambda\lambda$3726, 3729, He ii λ4686, Hβ and [O iii] λ5007 emission lines; the W-values of Ca ii K λ3933 ($W_{\rm K}$), CN λ4200 ($W_{\rm CN}$), and G band λ4301 ($W_{\rm G}$) absorption bands, the continuum fluxes at 3660, 4020, and 4510 Å, as well as the 12 μm and far-IR luminosities as measured by *IRAS*. These are listed in Tables 1 and 2, along with heliocentric velocities extracted from NED.[3] Table 2 also lists the Hα/Hβ ratio for the Seyfert 2 sample, mostly compiled from the literature, since the Kitt Peak spectra do not cover the Hα region. These measurements come from spectra obtained with apertures larger than those used in our observations. For this reason, and also because of the intrinsic uncertainties associated with reddening corrections, we will concentrate on reddening insensitive diagnostics inasmuch as possible. Galaxies which had hidden Seyfert 1 nuclei revealed through spectropolarimetry are indicated by the corresponding reference in the last column of Table 2.

All absorption line W-values and continuum fluxes used in this paper were measured according to the system explained in Cid Fernandes et al. (1998). Emission line and continuum fluxes were corrected for Galactic extinction following the extinction law of Cardelli, Clayton, & Mathis (1989, with $R_V = 3.1$), and A_B-values from Schlegel, Finkbeiner, & Davis (1998) as listed in NED.

2.1. *Composite and "Pure" Seyfert 2 Galaxies*

Fifteen of our Seyfert 2's have unambiguous evidence for starbursts as revealed by at least one of the three diagnostics outlined above. These are ESO 362-G8, IC 3639, Mrk 1, Mrk 78, Mrk 273, Mrk 477, Mrk 463E, Mrk 533, Mrk 1066, Mrk 1073, Mrk 1210, NGC 5135, NGC 5643, NGC 7130, and NGC 7582 (observed prior to the type transition reported in Aretxaga et al. 1999), which will henceforth be tagged *composite* systems. The circumnuclear starbursts in these galaxies cover a wide range of properties, from very young bursts still in the WR phase (e.g., Mrk 477, Mrk 1) to more mature systems in a "poststarburst" phase with deep high-order Balmer absorption lines (e.g., Mrk 78, ESO 362-G8), and systems which have a mixture of both young and intermediate-age stars (e.g., NGC 5135, NGC 7130).

The remaining 20 sources will be labeled "*pure*" Seyfert 2's. This denomination is used simply to indicate that no clear signs of starburst activity have been detected in our previous studies. The spectra among our "pure" Seyfert 2's vary from galaxies whose optical light is entirely dominated by an old, red stellar population (e.g., NGC 1358 and NGC 5929) to galaxies which show clear signs of an UV-excess (e.g., Mrk 3 and Mrk 348). It is nearly impossible to tell on the basis of optical spectra alone whether this FC is associated with scattered light, a starburst, or a combination of both. This point was discussed at length by SB00, who argue that as many as 30% of Seyfert 2's can fall in this ambiguous category. GD01 also finds that several galaxies are equally well described in terms of a scattered power-law or a starburst component, depending basically on what is chosen to represent the underlying old stellar population. Far-UV spectroscopy offers the best hope to break this degeneracy, but this is not practical with currently available instrumentation, so we will have to live with this ambiguity for some time. Indeed, this ambiguity pervades all discussions in this paper.

We emphasize that the composite and "pure" categories are *not* meant as new elements in the AGN taxonomy. It is clear that this classification reflects a *detectability* effect, since we define composites as systems in which stars with ages of 10^{6-8} yr have been conclusively detected. This definition therefore introduces an inevitable bias toward starbursts that are powerful in contrast with the other

[3] The NASA/IPAC Extragalactic Database (NED) is operated by the Jet Propulsion Laboratory, California Institute of Technology, under contract with the National Aeronautics and Space Administration.

TABLE 1

SEYFERT 2 SAMPLE: CONTINUUM, ABSORPTION, AND EMISSION LINE PROPERTIES

Galaxy (1)	W_K (2)	W_{CN} (3)	W_G (4)	F_{3660}/F_{4020} (5)	F_{4510}/F_{4020} (6)	$W_{[O\ II]}$ (7)	$W_{He\ II}$ (8)	$W_{H\beta}$ (9)	$W_{[O\ III]}$ (10)	$F_{[O\ II]}$ (11)	$F_{He\ II}$ (12)	$F_{[O\ III]}$ (13)	$F_{H\beta}$ (14)
CGCG420−015	14.0	9.7	8.4	0.53	1.67	32.5	4.7	16.9	208.5	7.9×10^{-15}	3.6×10^{-15}	1.7×10^{-13}	1.4×10^{-14}
ESO 417-G6	14.6	11.3	9.4	0.57	1.29	42.1		2.8	18.1	1.8×10^{-14}		2.3×10^{-14}	2.8×10^{-15}
ESO 362-G8[a]	7.3	6.6	5.9	0.35	1.21	3.2			13.1	4.2×10^{-15}		5.3×10^{-14}	
Fairall 316	17.2	14.2	11.3	0.61	1.59	30.1		1.4	22.2	8.8×10^{-15}		2.0×10^{-14}	1.2×10^{-15}
IC 1816	11.8	10.0	8.2	0.65	1.29	59.8	4.7	15.7	244.7	3.0×10^{-14}	4.9×10^{-15}	2.6×10^{-13}	1.8×10^{-14}
IC 3639[a]	8.0	4.6	5.4	0.67	1.07	40.3	2.8	16.2	122.6	4.4×10^{-14}	4.7×10^{-15}	2.1×10^{-13}	2.7×10^{-14}
IRAS 11215−2806	13.1	7.5	7.3	0.54	1.28	19.9	1.4	2.9	52.9	6.1×10^{-15}	1.1×10^{-15}	4.3×10^{-14}	2.2×10^{-15}
MCG -05-27-013	15.4	10.9	9.7	0.71	1.54	114.2	7.2	22.9	244.8	1.2×10^{-14}	2.0×10^{-15}	8.1×10^{-14}	7.0×10^{-15}
Mrk 1[a]	7.6	6.0	4.4	0.83	1.11	131.4	12.2	53.5	765.9	3.4×10^{-14}	4.8×10^{-15}	2.7×10^{-13}	2.2×10^{-14}
Mrk 3	11.3	10.2	6.7	1.04	1.38	263.4	12.3	67.8	752.7	4.9×10^{-13}	3.6×10^{-14}	3.0×10^{-12}	2.1×10^{-13}
Mrk 34	9.9	6.7	7.0	0.81	1.20	157.2	11.2	42.1	475.0	2.7×10^{-14}	2.7×10^{-15}	1.0×10^{-13}	1.0×10^{-14}
Mrk 78[a]	9.6	7.6	6.2	0.48	1.25	96.0	3.3	9.3	131.2	2.5×10^{-14}	2.3×10^{-15}	9.0×10^{-14}	6.6×10^{-15}
Mrk 273[a]	5.6	5.2	3.9	0.58	1.03	46.4		11.9	35.8	7.6×10^{-15}		7.9×10^{-15}	2.8×10^{-15}
Mrk 348	12.5	8.4	7.7	0.76	1.30	118.6	3.7	22.1	274.7	4.7×10^{-14}	2.8×10^{-15}	2.2×10^{-13}	1.7×10^{-14}
Mrk 463[a]	3.0	5.6	0.9	1.05	1.04	135.0	11.6	88.1	978.5	5.5×10^{-14}	4.7×10^{-15}	3.3×10^{-13}	3.8×10^{-14}
Mrk 477[a]	0.3	2.4	0.2	1.10	0.98	168.1	13.2	92.5	743.2	7.6×10^{-14}	6.4×10^{-15}	4.5×10^{-13}	4.5×10^{-14}
Mrk 533[a]	4.1	3.1	3.1	0.68	1.06	49.8	9.2	36.3	429.2	2.2×10^{-14}	6.1×10^{-15}	2.2×10^{-13}	2.1×10^{-14}
Mrk 573	14.1	11.8	9.0	0.67	1.44	83.2	9.2	20.6	282.7	4.9×10^{-14}	1.1×10^{-14}	3.1×10^{-13}	2.5×10^{-14}
Mrk 607	13.8	12.3	9.9	0.61	1.43	19.1	4.0	7.1	78.1	8.6×10^{-15}	4.5×10^{-15}	9.5×10^{-14}	8.0×10^{-15}
Mrk 1066[a]	5.6	4.3	3.5	0.75	1.03	43.9	2.3	24.3	93.1	5.9×10^{-14}	4.1×10^{-15}	1.6×10^{-13}	4.2×10^{-14}
Mrk 1073[a]	5.7	5.4	4.7	0.74	1.06	40.2	5.1	19.9	122.1	3.2×10^{-14}	5.7×10^{-15}	1.3×10^{-13}	2.2×10^{-14}
Mrk 1210[a]	7.5	7.6	5.5	0.83	1.20	59.3	8.8	57.0	614.0	4.1×10^{-14}	9.5×10^{-15}	5.6×10^{-13}	5.5×10^{-14}
NGC 1068	7.4	7.7	5.1	0.72	1.26	33.4	11.6	35.0	343.7	3.2×10^{-13}	1.9×10^{-13}	7.3×10^{-12}	5.6×10^{-13}
NGC 1358	17.8	16.1	11.5	0.54	1.50	17.8		0.9	19.7	9.4×10^{-15}		3.2×10^{-14}	1.4×10^{-15}
NGC 1386	13.2	9.0	8.1	0.54	1.56	25.5	2.5	3.4	58.8	2.3×10^{-14}	6.8×10^{-15}	1.6×10^{-13}	9.2×10^{-15}
NGC 2110	13.5	12.8	8.9	0.78	1.31	177.6	2.0	15.8	78.3	8.6×10^{-14}	1.9×10^{-15}	8.1×10^{-14}	1.6×10^{-14}
NGC 3081	13.7	10.5	8.7	0.69	1.38	36.6	4.9	9.3	128.0	7.9×10^{-15}	2.3×10^{-15}	6.6×10^{-14}	4.7×10^{-15}
NGC 5135[a]	2.5	1.7	2.5	0.77	0.87	20.6	1.8	13.2	51.3	4.5×10^{-14}	4.1×10^{-15}	1.1×10^{-13}	2.7×10^{-14}
NGC 5643[a]	9.4	4.2	4.6	0.50	1.24	56.4	2.8	8.7	115.0	5.7×10^{-14}	6.8×10^{-15}	2.7×10^{-13}	1.9×10^{-14}
NGC 5643[a]	9.4	4.2	4.6	0.50	1.24	56.4	2.8	8.7	115.0	3.0×10^{-13}	3.5×10^{-14}	1.4×10^{-12}	1.0×10^{-13}
NGC 5929	14.3	11.0	9.6	0.71	1.39	107.0	1.6	14.5	58.5	3.9×10^{-14}	1.2×10^{-15}	5.0×10^{-14}	1.2×10^{-14}
NGC 6300	15.9	4.0	5.8	0.49	1.64	15.9			27.9	3.3×10^{-15}		2.4×10^{-14}	
NGC 6890	12.6	1.0	4.8	0.72	1.42	16.5	2.4	3.9	74.2	4.5×10^{-15}	1.3×10^{-15}	4.4×10^{-14}	2.2×10^{-15}
NGC 7130[a]	3.7	2.2	2.4	0.73	1.00	24.8	2.3	14.8	104.0	1.4×10^{-14}	1.8×10^{-15}	7.3×10^{-14}	1.1×10^{-14}
NGC 7212	10.4	8.1	6.9	0.92	1.33	211.2	13.8	55.2	725.5	7.0×10^{-14}	7.0×10^{-15}	3.5×10^{-13}	3.0×10^{-14}
NGC 7582[a]	3.7	3.1	3.0	0.55	1.23	19.2	1.6	15.2	33.0	1.3×10^{-14}	2.6×10^{-15}	5.6×10^{-14}	2.4×10^{-14}

NOTES.—Absorption line, continuum, and emission line properties for the Seyfert 2 Sample, all extracted through small apertures (1.2″ × 2.1″ or 2″ × 2″). All equivalent widths are given in Å and line fluxes in ergs s^{-1} cm^{-2} (after correction for Galactic extinction). Empty slots correspond to weak lines, which were not measured. The flux calibration for NGC 5643, NGC 6300, and NGC 6890 are very uncertain due to weather conditions. Table 1 is also available in machine-readable form in the electronic edition of the *Astrophysical Journal*.

[a] Confirmed starburst/Seyfert 2 composite.

TABLE 2

SEYFERT 2 SAMPLE: ADDITIONAL DATA

Galaxy (1)	$A_{B,\mathrm{Gal}}$ (2)	cz (3)	Hα/Hβ (4)	log $L_{12\mu}$ (5)	log L_{FIR} (6)	log $L_{\mathrm{H}\beta}$ (7)	Ref. (8)	Ref. (9)
CGCG420−015	0.37	8811	5.5	10.43	9.76	40.37	dG92	
ESO 417-G6	0.09	4884	4.7	9.29	8.45	39.16	S98	
ESO 362-G8[a]	0.14	4785		9.34	9.16			
Fairall 316	0.60	4950	6.4			38.80	S98	
IC 1816	0.12	5080	6.0	9.75	10.03	39.98	dG92	
IC 3639[a]	0.30	3275	6.1	9.98	10.35	39.79	dG92	H97
IRAS 11215−2806	0.31	4047	3.8	9.56	9.08	38.88	dG92	
MCG -05-27-013	0.28	7162	5.0	9.75	9.99	39.88	dG92	
Mrk 1[a]	0.26	4780	5.9	10.47	10.18	40.03	M94	
Mrk 3	0.81	4050	6.6	10.21	10.18	40.86	M94	MG90, T95
Mrk 34	0.04	15140	10.5	10.33	10.66	40.69	M94	
Mrk 78[a]	0.15	11137	6.5	10.34	10.39	40.24	M94	
Mrk 273[a]	0.04	11326	9.3	10.62	11.84	39.88	M94	
Mrk 348	0.29	4507	6.0	9.94	9.84	39.86	M94	MG90, T95
Mrk 463E[a]	0.13	14895	5.6	11.19	11.07	41.25	M94	MG90, T95
Mrk 477[a]	0.05	11332	5.4	10.35	10.67	41.09	M94	T95
Mrk 533[a]	0.25	8713	5.0	10.85	11.08	40.54	M94	MG90, T95, H97
Mrk 573	0.10	5174	4.2	9.66	9.88	40.16	M94	K94
Mrk 607	0.20	2716	4.9	9.53	9.63	39.10	D88	
Mrk 1066[a]	0.57	3605	8.5	9.90	10.56	40.06	M94	
Mrk 1073[a]	0.69	6998	6.3	10.48	11.04	40.35	M94	
Mrk 1210[a]	0.13	4046	5.2	10.05	9.85	40.28	B99	T95
NGC 1068	0.14	1137	4.5	10.85	10.79	40.18	M94	AM85
NGC 1358	0.27	4028	3.4	8.95	9.34	38.69	M94	
NGC 1386	0.05	868	4.9	8.71	9.09	38.17	M94	
NGC 2110	1.62	2335	8.1	9.42	9.79	39.28	M94	
NGC 3081	0.24	2385	4.5			38.75	M94	M00
NGC 5135[a]	0.26	4112	6.1	10.17	10.93	39.99	M94	
NGC 5643[a]	0.73	1199	6.2	9.34	9.95	38.77	M94	
NGC 5929	0.10	2492	6.2	9.57	10.21	39.21	M94	
NGC 6300	0.42	1110		9.20	9.80			
NGC 6890	0.17	2419	4.2	9.44	9.87	38.43	M94	
NGC 7130[a]	0.12	4842	6.6	10.28	11.05	39.73	S98	
NGC 7212	0.31	7984	5.0	10.24	10.74	40.61	M94	T95
NGC 7582[a]	0.06	1575	8.3	9.74	10.54	39.11	M94	

NOTES.—Col. (1): Object name. Col. (2): Galactic B-band extinction (from NED). Col. (3): cz in km s^{-1}. Col. (4): Balmer decrement (compiled from the literature). Col. (5): νL_ν at 12 μm from *IRAS*, in $L_\odot$. Col. (6): Far-IR luminosity in $L_\odot$ computed with the *IRAS* 60 and 100 μm fluxes using the formula in Sanders & Mirabel 1996. When only upper limits were available for the *IRAS* fluxes we use half the quoted limit to compute fluxes. Col. (7): Hβ luminosity in ergs s^{-1}, corrected only for Galactic extinction. Col. (8): Reference for the Balmer decrement. Col. (9): References regarding spectropolarimetry detection of hidden Seyfert 1 nucleus.

[a] Confirmed starburst/Seyfert 2 composite.

REFERENCES.—(AM85) Antonucci & Miller 1985; (B99) Bassani et al. 1999; (D88) Dahari & De Robertis 1988; (dG92) de Grijp et al. 1992; (H97) Heisler, Lumsden, & Bailey 1997; (K94) Kay 1994; (M00) Moran et al. 2000; (M94) Mulchaey et al. 1994; (MG90) Miller & Goodrich 1990; (S98) Schmitt 1998; (T95) Tran 1995a, 1995b.

components of Seyfert 2 spectra, a bias which will become evident in several of the results presented in this paper. While it is likely that some "pure" sources eventually be "upgraded" to composites with deeper or different observations (e.g., when far-UV spectra are obtained, or when near-IR mass to light ratios are measured), it is unlikely that any of the composites will ever be reclassified as a "pure" Seyfert 2. Until such further notice, all galaxies not in the list of 15 composites above will be designated "pure" Seyfert 2's.

The composite/"pure" classification will be used throughout this paper as a guide to interpret our results, even though we shall *not* make explicit use of any of the properties on which this classification is based. Instead, we seek to find where composite sources fit into more general and easily accessible properties of Seyfert 2's.

2.2. *Comparison Samples*

As comparison samples we draw data from three different observational studies. The first is the spectroscopy of 61 Starburst and narrow line active galaxies (NLAGNs) by Storchi-Bergmann, Kinney, & Challis (1995) and McQuade, Calzetti, & Kinney (1995, hereafter collectively referred to as SBMQ95). The Starburst galaxies in their study will be referred to as the "Starburst sample," which will be extensively used as a benchmark when gauging the results for our Seyfert 2's. UGCA410 was removed from our analysis because of apparently incompatible values of W_{K} and W_{G}, leaving a total of 36 Starburst galaxies. The remaining 24 sources in SBMQ95 contain a mixture of Seyfert 2's, LINERs, and starburst/AGN composites, so we give them a generic denomination of "NLAGN sample." In principle

these galaxies serve as a test bed to evaluate the efficacy of the diagnostics of compositeness developed from our Seyfert 2 sample. In practice, we will make limited use of this sample because of the mixed nature of its sources, which complicates the interpretation. Galaxies in the Starburst and NLAGN samples were observed with very large $10'' \times 20''$ apertures to match the *IUE* observations, sampling physical scales of typically ~ 1 kpc in radius at the distances of the sources.

A third comparison sample used here is the "merger sample" from the study of Liu & Kennicutt (1995a, 1995b, hereafter LK95). This sample comprises 28 nuclear optical spectra integrated over a region corresponding to ~ 0.5–2 kpc in radius. The emission line properties of these galaxies are quite heterogeneous, comprising five Seyfert 2's, nine H II nuclei, and 14 LINERs. Lutz, Veilleux, & Genzel (1999) have used ISO data to show that IR-luminous galaxies with H II or LINER classifications are predominantly powered by starbursts, while dusty AGNs are energetically significant in those classified as Seyfert 2's. Thus, we will use the merger sample to empirically define the properties of powerful merger-induced dusty starbursts.

The data which will be used from these samples consist of fluxes and W-values of [O II], Hβ and [O III]; W_K, W_{CN}, and W_G, plus the continuum fluxes at 3660, 4020, and 4510 Å and *IRAS* fluxes. Both the SBMQ95 and LK95 data offer more information than this, but we shall limit our analysis to the properties above for consistency with the Seyfert 2 sample.

Figure 1 shows the projected aperture radii, defined as $r_{ap} = (\text{slit area}/\pi)^{1/2}$, against W_K for the Seyfert 2, NLAGN, Starburst, and merger samples. Though the physical region sampled in the comparison samples extend well beyond that covered by the nuclear spectra of the Seyfert 2 sample, there is some overlap at small r_{ap} which guarantees the fairness of the comparisons presented in this paper, and in any case aperture effects will be discussed whenever relevant.

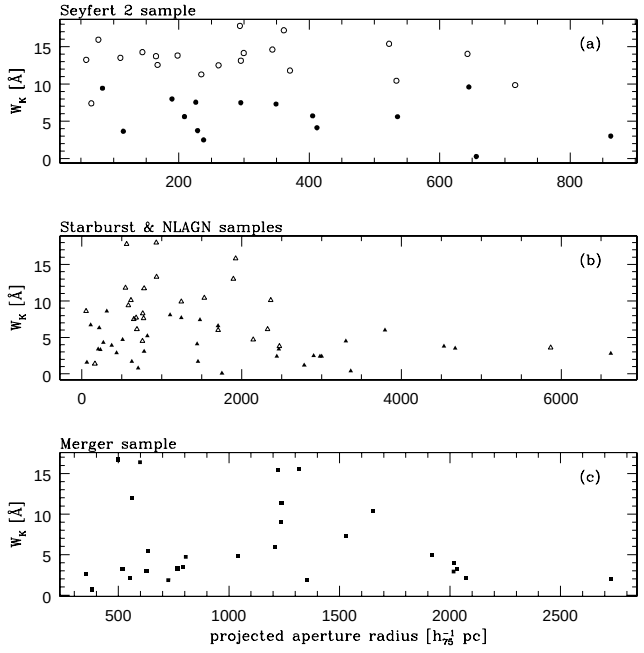

FIG. 1.—Aperture radii against the equivalent width of Ca II K for the Seyfert 2 (*a*), Starburst and NLAGN (*b*), and merger (*c*) samples. Open and filled circles in panel (*a*) indicate "pure" and composite Seyfert 2's, respectively. Open triangles in (*b*) correspond to NLAGN sources, whereas filled triangles correspond to Starburst galaxies.

Figure 1*a* also shows that the composite classification is *not* related to the physical size of the region sampled by our spectra. In principle one would expect that systems observed through larger apertures are more prone to exhibit starburst features due to the inclusion of light from off-nuclear star-forming regions. This effect has been quantified by Heckman et al. (1995) in their analysis of the aperture dependent properties of NGC 1068, whose 1 kpc ring of H II regions dominates the light for observations taken through kiloparsec-scale apertures. Such rings are in fact rather common (e.g., Pogge 1989; Wilson et al. 1991; Storchi-Bergmann, Wilson, & Baldwin 1996; Colina et al. 1997) and thus can play a role in defining a composite nature for more distant objects, as also discussed by Heckman et al. (1995). If such aperture effects were pronounced in the Seyfert 2 sample, we would expect composites to be concentrated toward large r_{ap}, whereas Figure 1*a* shows that composites and "pure" Seyfert 2's are similarly distributed as a function of r_{ap}. Furthermore, most of the apertures for the Seyfert 2 sample are much smaller than the 1 kpc typical of star-forming rings. This effect does not affect the Seyfert 2 sample, as our circumnuclear starbursts are relatively compact ($\sim$few hundred pc). These dimensions have in fact been confirmed by *HST* UV imaging for Mrk 477 (Heckman et al. 1997), NGC 5135, NGC 7130, and IC 3639 (González Delgado et al. 1998) and are comparable to the inner star-forming structures identified in the Circinus galaxy (Wilson et al. 2000). A further example of how compact circumnuclear starbursts around AGNs can be is given in Shields et al. (2000).

Another data set that will be used in this paper is that of Jansen et al. (2000). This sample contains multicolor surface photometry for 198 galaxies, most of which classified as normal. We used their data to calculate the 3660 Å surface brightness of these galaxies inside radii of 250 and 500 pc, similar to the apertures used for our galaxies. These values are used to compare the UV surface brightness of Seyfert and normal galaxies. The four Seyfert 1 and one BL Lac in their sample were excluded from our analysis.

3. ANALYSIS OF THE STARLIGHT AND THE FEATURELESS CONTINUUM IN SEYFERT 2 GALAXIES

Determining the FC contribution to the optical spectrum of Seyfert 2's is an important but difficult task, for which there is no definitive recipe. The traditional and still most widely employed method, which dates back to at least Koski (1978), is to remove the contribution of the old red stars from the host's bulge by adopting an elliptical or early-type spiral normal galaxy as a spectral template. The spectral decomposition is accomplished by assuming a $F_\nu \propto \nu^{-\alpha}$ power law for the "nonstellar" FC, whose strength is then adjusted to minimize the residuals, yielding typically $\alpha = 1$–2. Naturally, this procedure precludes the detection of young stellar populations, whose most conspicuous optical absorption features are masked by emission lines even in starburst galaxies. Furthermore, there is no simple way to tell apart a power-law FC from that produced by a reddened starburst (e.g., Cid Fernandes & Terlevich 1995). Only upon careful scrutiny of high-quality spectra is it possible to discern the presence of a starburst

from its high-order Balmer lines or, sometimes, the WR bump (see discussion in GD01). Therefore, *the FC strength will in general include a contribution from young stars as well as a bona fide nonstellar FC*, composed of scattered light from the hidden nucleus plus nebular continuum.

"Featureless" is of course a misnomer for a spectral component at least partly associated with starlight. We nonetheless retain this terminology both for historical reasons and because to first order a young stellar population does produce weak spectral features in the optical range. When referring to scattered light from the hidden nucleus we will use the term "FC1" introduced by Tran (1995c). As argued by Cid Fernandes & Terlevich (1995), Heckman et al. (1995), and Tran (1995c), strong FC Seyfert 2's must also contain another source of FC photons, "FC2" in Tran's notation, to account for the absence of conspicuous broad lines and the larger polarizations observed in the reflected broad lines than in the reflected nuclear continuum. At least for the composite systems, there is little doubt that FC2 is associated with circumnuclear starbursts (see GD01). Nebular continuum and emission from the scattering region itself (Tran 1995c) are other possible contributors to FC2.

In this paper we explore a different way to determine the FC strength. We decompose the total light into a base of 12 simple stellar population components represented by star clusters spanning the 10^6 to 10^{10} yr age range and different metallicities (Schmidt et al. 1991; Bica 1988), plus a $v^{-1.5}$ power law to represent FC1 and any other AGN component. This is done by means of a population synthesis analysis similar to that employed by Schmitt et al. (1999), but performed with the probabilistic formalism described in Cid Fernandes et al. (2001), extended to include the power-law component. Note that this method is analogous, but not technically equivalent to, a full spectral decomposition as only a few W-values and colors are actually synthesized. As input data we use the W-values of Ca II K, CN, and G band, plus the F_{3660}/F_{4020} and F_{4510}/F_{4020} colors. The errors on these quantities were set to 0.5 Å for W_K and W_G, 1 Å for W_{CN}, and 0.05 for the colors; these errors are consistent with the quality of the spectra, and in any case they do not affect our conclusions. The output is a 13-D population vector $\boldsymbol{x}$ which contains the expected values of the fractional contribution of each component to the total light at a reference normalization wavelength. In what follows we shall use 4861 Å as our reference wavelength unless noted otherwise. Uncertainties in $\boldsymbol{x}$ are also provided by the code.

It is clear from the outset that with so little input information we will not be able to recover all 13 components of $\boldsymbol{x}$ accurately, but, as discussed by Cid Fernandes et al. (2001), we may rightfully hope to achieve a coarse yet useful description of the population mixture by grouping similar elements of the population vector. In what follows we shall make use of only three grouped $\boldsymbol{x}$ components: x_{OLD}, made up from the sum of all base components with age ≥ 1 Gyr, x_{INT}, corresponding to the "poststarburst" 10^8 yr intermediate-age bin, and, most importantly for our purposes, x_{FC}, containing the total contribution of $\leq 10^7$ yr stars plus the power-law component. These quantities are linked by the $x_{OLD} + x_{INT} + x_{FC} = 1$ normalization constraint, so in practice our method characterizes the spectral mixture in terms of *two parameters*. This biparametric description of the data is in many ways analogous to a principal component analysis (Sodré & Cuevas 1997; Rodrigues-Lacerda 2001), except that by construction we have a priori knowledge of the physical meaning of our components.

Note that *we do not attempt to disentangle the starburst and power-law components* explicitly; these are merged in $x_{FC} = x_{YS} + x_{PL}$, where x_{YS} and x_{PL} stand for the light fractions due to young ($\leq 10^7$ yr) stars and the power law, respectively. As shown below, both the FC strength and the emission line properties give us strong hints as to which of these two components dominates x_{FC}, thus helping to break this degeneracy.

3.1. *Results of the Synthesis*

The results of this analysis are listed in Table 3 in order of decreasing x_{FC}. A first noticeable result in this table is that composites are concentrated toward the top of the list: All 10 $x_{FC} \geq 29\%$ sources are confirmed Seyfert 2/starburst composites, and 12 of the 15 composites are among the 16 sources with $x_{FC} > 15\%$ at 4861 Å. The identification of x_{FC} with x_{YS} (i.e., $x_{YS} \gg x_{PL}$) is thus safe for these objects.

TABLE 3

SYNTHESIS RESULTS

Galaxy (1)	x_{OLD} (%) (2)	x_{INT} (%) (3)	x_{FC} (%) (4)
Mrk 477[a]	10.5 ± 3.4	2.8 ± 2.0	86.6 ± 4.2
Mrk 463E[a]	27.7 ± 4.3	3.8 ± 2.5	68.5 ± 4.0
NGC 5135[a]	27.2 ± 7.3	26.9 ± 6.2	45.9 ± 5.8
NGC 7130[a]	36.3 ± 8.0	23.6 ± 6.1	40.1 ± 5.9
Mrk 533[a]	40.9 ± 7.7	25.3 ± 6.1	33.8 ± 5.5
Mrk 1066[a]	51.5 ± 6.8	16.3 ± 5.4	32.3 ± 4.9
NGC 7582[a]	35.6 ± 7.8	33.8 ± 6.5	30.6 ± 5.7
Mrk 1[a]	63.1 ± 5.6	7.1 ± 3.6	29.8 ± 4.0
Mrk 1073[a]	55.3 ± 6.2	15.6 ± 5.1	29.1 ± 4.6
Mrk 1210[a]	65.1 ± 4.7	5.9 ± 3.1	29.0 ± 3.5
NGC 1068	63.2 ± 5.5	11.1 ± 4.3	25.7 ± 4.0
Mrk 3	77.8 ± 2.7	1.1 ± 0.8	21.1 ± 2.0
NGC 7212	77.3 ± 3.6	2.0 ± 1.4	20.8 ± 2.6
Mrk 273[a]	47.3 ± 7.1	34.8 ± 6.2	17.9 ± 4.7
Mrk 34	78.1 ± 4.6	4.1 ± 2.5	17.7 ± 3.1
IC 3639[a]	69.9 ± 6.8	14.4 ± 5.0	15.7 ± 4.1
Mrk 348	87.2 ± 4.4	3.2 ± 2.0	9.7 ± 2.6
NGC 2110	87.8 ± 3.4	2.5 ± 1.6	9.6 ± 2.0
IC 1816	84.5 ± 4.8	7.2 ± 3.3	8.3 ± 2.6
NGC 5643[a]	73.2 ± 7.2	19.5 ± 5.3	7.3 ± 3.2
Mrk 78[a]	72.0 ± 6.5	21.2 ± 4.9	6.8 ± 2.9
NGC 3081	90.1 ± 4.3	3.4 ± 2.0	6.4 ± 2.1
Mrk 573	90.9 ± 4.3	3.4 ± 2.0	5.6 ± 1.9
NGC 5929	91.7 ± 3.7	2.7 ± 1.7	5.6 ± 1.9
NGC 6890	93.1 ± 4.5	1.9 ± 1.4	5.0 ± 2.2
NGC 1386	89.9 ± 5.4	5.1 ± 2.7	5.0 ± 2.1
Mrk 607	90.4 ± 4.4	4.7 ± 2.4	4.9 ± 1.8
ESO 362-G8[a]	56.6 ± 5.9	38.5 ± 4.9	4.9 ± 2.4
CGCG 420−015	91.7 ± 5.0	4.1 ± 2.3	4.2 ± 1.8
MCG -05-27-013	93.9 ± 3.7	1.9 ± 1.3	4.2 ± 1.6
IRAS 11215−2806	90.0 ± 5.7	5.9 ± 3.0	4.0 ± 1.9
ESO 417-G6	92.7 ± 4.6	4.0 ± 2.2	3.3 ± 1.5
Fairall 316	96.6 ± 3.8	1.5 ± 1.0	1.9 ± 0.9
NGC 6300	96.5 ± 4.6	1.7 ± 1.2	1.8 ± 1.0
NGC 1358	97.6 ± 3.8	1.2 ± 0.8	1.2 ± 0.7

NOTES.—Col. (1): Object name. Cols. (2–4): Fractions of the total light at 4861 Å due to old stars (x_{OLD}), 100 Myr stars (x_{INT}); and ≤ 10 Myr old stars plus a $v^{-1.5}$ power-law FC (x_{FC}). Galaxies are organized in order of descending FC strength.

[a] Confirmed starburst/Seyfert 2 composites.

An even more remarkable result is that *all* 15 composites but *only one* "pure" Seyfert 2 (NGC 1068) have $x_{OLD} < 75\%$. This is illustrated in Figure 2*a*, where we condense the results of the synthesis in the $x_{FC} \times x_{INT}$ plane, with dotted lines indicating lines of constant $x_{OLD} = 1 - x_{INT} - x_{FC}$. *The diagram segregates composite from "pure" systems very effectively*, and it does so in agreement with what one would expect: composites have larger proportions of intermediate-age and young stars, the latter being included in x_{FC}.

As a check on our method, we have applied it to the spectra in the comparisons samples, which, for consistency, were processed in exactly the same way as our Seyfert 2's. If our method works, we would expect bona fide Starburst galaxies to be located within the $x_{OLD} < 75\%$ zone, probably more toward even lower values of x_{OLD}, overlapping with our more extreme composites. This is confirmed in Figure 2*b*, which shows the synthesis results for the Starburst, merger, and NLAGN samples. There is not a single Starburst galaxy (*filled triangles*) for which $x_{OLD} > 65\%$, whereas most of the NLAGNs are located there. Furthermore, most of the NLAGNs which intrude into the starburst region are known starburst/Seyfert 2 composites! The four open triangles in the $x_{OLD} < 50\%$ zone, for instance, are Mrk 477, NGC 5135, NGC 7130 (all also in our Seyfert 2 sample), and NGC 7496, whose composite nature is discussed in Véron, Gonçalves & Véron-Cetty (1997). The $50\% < x_{OLD} < 75\%$ zone also contains known composites, both from our sample (IC 3639 and NGC 7582), and from independent work, such as NGC 4569 (Keel 1996; Maoz et al. 1998), NGC 1672 (Véron et al. 1997), and NGC 6221 (Levenson et al. 2001a).

As expected, most of the sources in the merger sample (Fig. 2*b*, *squares*) behave like starbursts in our stellar population diagram. Note that our synthesis indicates a strong contribution of $\sim 10^8$ yr populations for most sources in this sample. This is consistent with the results of LK95, who find a high incidence of systems in a poststarburst phase based on the detection of the Balmer absorption series. Those mergers which are dominated by old stars ($x_{OLD} > 50\%$) are predominantly LINERs (e.g., NGC 942, NGC 3656, and 3C 293).

It is thus clear that, despite its limitations, our biparametric description of the data provides a very efficient empirical diagnostic of compositeness in Seyfert 2's. Since our operational definition of composites is based on the detectability of starburst features, which is certainly facilitated when they make a strong contribution to the continuum, the result that sources with large x_{FC} and/or x_{INT} are mostly composites is somewhat redundant. The importance of this result is twofold. First, it shows a striking empirical similarity between the bona fide starburst galaxies (whose optical/near-UV continuum is definitely produced by young and intermediate-age stars) and the starburst/Seyfert 2 composites. Second, it demonstrates an excellent *consistency* between the two techniques, which are based on different observables. The synthesis process did *not* use any of the information used in the original identification of starbursts in these composites, namely, far-UV stellar wind features, high-order Balmer lines, and/or the WR bump, all of which are much more subtle or hard to obtain than the observables used as input for the synthesis code.

3.2. *Contrast and Evolution*

The separation between composites and "pure" Seyfert 2's in Figure 2*a* strongly suggests that, as anticipated in § 2.1, the composite/"pure" classification is mostly driven by a *contrast* effect: Systems with circumnuclear starbursts residing in galaxies where the old stellar population dominates the spectrum would simply not be recognized as composite systems. This contrast effect is nicely quantified by the value of x_{OLD}, which can therefore be read as a measure of the difficulty to detect any nontrivial spectral component

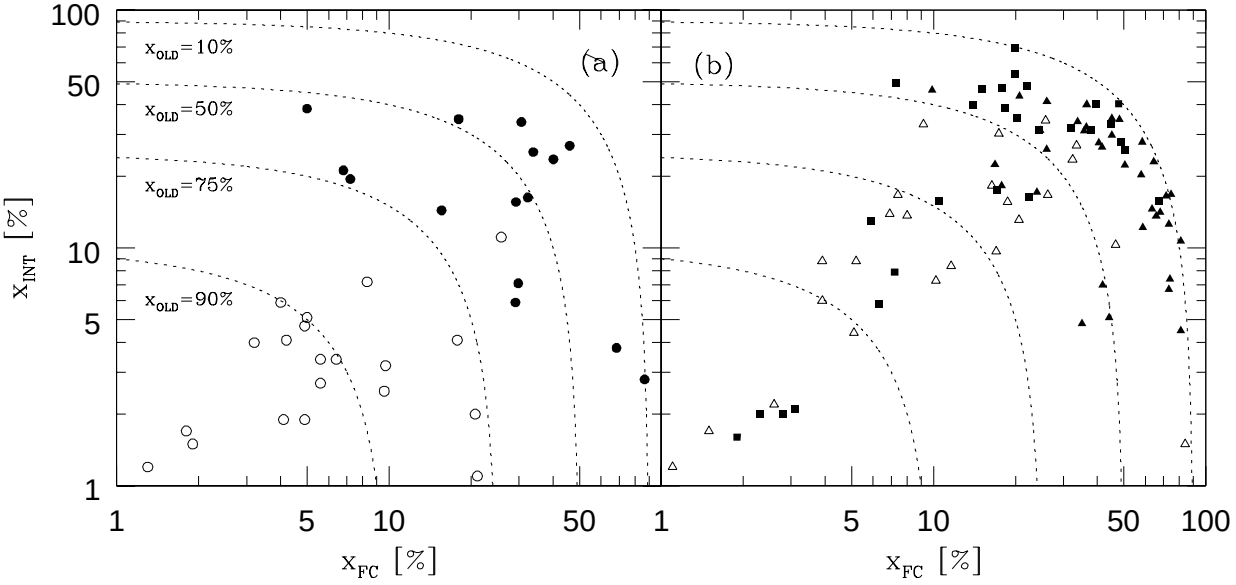

FIG. 2.—Results of the synthesis analysis, condensed into a biparametric x_{FC} and x_{INT} representation. Dotted lines trace lines of constant x_{OLD}, as labeled. (*a*) Sources from the Seyfert 2 sample, with filled circles indicating the starburst/Seyfert 2 composites. The open circle among the $x_{OLD} < 75\%$ zone otherwise exclusively occupied by composites is NGC 1068. As x_{OLD} increases it becomes progressively difficult to detect starburst features in Seyfert 2's, explaining the clear separation between composites and "pure" Seyfert 2's in this diagram. (*b*) Results for the Starburst (*filled triangles*), NLAGN (*open triangles*), and merger (*filled squares*) samples.

and to interpret its origin. Figure 2 shows that our current techniques establish a threshold of $x_{OLD} \sim 75\%$, beyond which we are not able to recognize circumnuclear starbursts. For instance, if we scale down the circumnuclear starburst in IC 3639 by a factor ≥ 2, it would move from $x_{OLD} = 70\%$ to more than 82%, where, judging by Figure 2, we would classify it as a "pure" Seyfert 2. It is therefore likely that at least some "pure" Seyfert 2's are just that: composites with weak starbursts.

The presence of strong H I emission lines introduces another contrast effect, since they dilute the high-order Balmer absorption lines, thus hindering the use of this diagnostic of starbursts. Therefore, *the combination of strong emission lines and a large x_{OLD} is highly unfavorable to the detection of circumnuclear starbursts.* We will return to this issue in § 4.1.1, after we analyze the emission line data.

Besides the contrast between the starburst and the underlying old stellar population, *evolution* is the main property defining the location of a source in Figure 2. One can easily imagine an evolutionary sequence which starts at some large value of x_{FC} in the bottom right part of the diagram, with massive young starts dominating the spectrum and no intermediate-age population, and gradually moves toward large x_{INT}/x_{FC} (i.e., to the top left of the diagram) on $\sim 10^8$ yr timescales. The exact shape of evolutionary tracks in our $x_{FC} \times x_{INT}$ diagram is dictated by the detailed star formation history, but for the purposes of the qualitative discussion below one can imagine that such tracks broadly follow the dotted lines traced in Figure 2 up to a few hundred Myr and then collapse to the origin, after the starburst ends and its stars move into our old population bin.

Here too we find a remarkable agreement between the present synthesis analysis and the results of our previous work on the composites in the Seyfert 2 sample. The four composites with largest x_{FC}/x_{INT} are Mrk 477, Mrk 463E, Mrk 1210, and Mrk 1 (going upward in Fig. 2*a*). These are precisely the four systems where we have identified WR stars (Heckman et al. 1997; Storchi-Bergmann et al. 1998; GD01), signposts of very recent star formation. They therefore rank as the youngest circumnuclear starbursts among our composites, in agreement with their location in Figure 2*a*. At the other extreme, the three composites with $x_{FC} < 10\%$ are NGC 5643, Mrk 78, and ESO 362-G8, all of which present spectroscopic signatures of a dominant "poststarburst" population (Schmitt et al. 1999; SB00; GD01) and rank as our oldest composites, in agreement with the large x_{INT} but small x_{FC} we obtain. Given this agreement at the young and old ends of a starburst evolutionary sequence, we would expect that systems located at x_{FC}/x_{INT}-values in between these extremes present a mixture of young and intermediate-age stars. This is indeed the case. The cluster of four composites toward the top right in Figure 2*a*, for instance, contains NGC 5135, NGC 7130, NGC 7582, and Mrk 533, all of which reveal spectroscopic signatures of this mixture (SB00; GD01), such as pronounced high-order Balmer absorption lines simultaneous with far-UV stellar wind lines.

What makes this agreement remarkable is the fact that while the characterization of the starburst component in our earlier work involved a detailed spectroscopic analysis, the synthesis performed here used just three W-values of metallic absorption bands plus a couple of near-UV colors. Our quicker and cheaper method is therefore not only able to recognize composite systems from a handful of easily measured observables, but it allows us to go one step further to provide a rough description of evolutionary state of the starburst component.

We will return to the issue of evolution in § 7. Before that, we have to deal with the contribution of the nonstellar FC in x_{FC}. This issue was deliberately omitted from the discussion above because we do *not* have a recipe to separate the stellar and nonstellar parts of the FC, neither do we know how or whether the nonstellar FC evolves on timescales comparable to the starburst lifetime. These difficulties limit considerations about evolution to composites alone, for which we know that the starburst component is the dominant contributor to the FC.

3.3. *The FC Component*

Our inability to disentangle the starburst and nonstellar components of the FC is currently the major obstacle to a full characterization of the starburst-AGN connection in Seyfert 2's. Unfortunately, these are also the most relevant spectral components in Seyfert 2's. The starburst portion of x_{FC} traces the ongoing star formation, being therefore associated with young massive stars which may have a significant impact on the ionization of the gas in the circumnuclear environment. On the other hand, the nonstellar component (which is presumably mainly scattered light, i.e., FC1) is the only continuum feature associated with the AGNs in these galaxies. For these reasons we concentrate on the FC component throughout most of the rest of this paper. Whereas little can be said about the starburst and AGN shares of x_{FC} in "pure" Seyfert 2's, composite systems have their FC dominated by the starburst (GD01; SB00) and hence provide a useful guide as to what can be deduced from the FC strength alone.

3.3.1. *Strong FC Sources Are Seyfert 2/Starburst Composites*

Table 3 shows that strong FC sources ($x_{FC} \gtrsim 30\%$) are likely to be composite systems. Within the context of the unified model, it is not surprising to find that a starburst component dominates over FC1 whenever the total FC is strong, since scattered light cannot exceed a fraction of $\sim 30\%$, otherwise reflected broad lines should become easily discernible in the direct spectrum and the galaxy would no longer be classified as a type 2 Seyfert. For a typical W of ~ 100 Å for broad Hβ in Seyfert 1's (Goodrich 1989; Binette, Fosbury, & Parker 1993), more than 30% scattered light would imply a broad Hβ stronger than 30 Å in the direct total spectrum. Cid Fernandes & Terlevich (1995) argue that broad lines should be seen even for smaller x_{FC1}, but we figure 30% is a reasonable limit in practice because NGC 1068 has $x_{FC} = 26\%$, and broad lines have not been conclusively detected there without the hindsight of spectropolarimetry to guide the eye (Miller & Goodrich 1990; Tran 1995b; Malkan & Filippenko 1983).

In support of this conclusion, we note that several cases of strong FC sources reported in the literature turned out to harbor starbursts not accounted for in the classical starlight template decomposition. For instance, Miller & Goodrich (1990) find $x_{FC} = 100\%$ in Mrk 463E, while GD01 suggest it actually contains a powerful starburst in the WR phase. The same can be said about Mrk 477, for which Tran (1995a, 1995b) finds $x_{FC} = 59\%$ at 5500 Å, and Mrk 1066, for which Miller & Goodrich (1990) find a 72% FC at 5300 Å. Even in Cygnus A, whose blue FC has remained a mystery for more

than a decade (e.g., Goodrich & Miller 1989; Tadhunter, Scarrott, & Rolph 1990), there now seems to be evidence for young stars (Fosbury et al. 1999). Indeed, inspection of the Keck spectrum in Ogle et al. (1997) even indicates the presence of a possible WR bump! This is consistent with our conclusion, since estimates of the FC strength for Cygnus A place it above the 30% level (Osterbrock 1983).

This high "success" rate suggests that one can *predict* the existence of circumnuclear starbursts based only on the FC strength. Despite the nonuniformity of FC estimation methods, one can be fairly confident that a search for sources with $x_{FC} > 30\%$ reported in the literature should identify other composite systems. Kay (1994), for instance, reports the following Seyfert 2's with an FC stronger than 30% at 4400 Å: Mrk 266SW (30%), Mrk 1388 (45%), NGC 591 (46%), NGC 1410 (38%), NGC 1685 (38%), NGC 4922B (53%), NGC 7319 (35%), NGC 7682 (30%). Koski (1978) finds a 34% FC at 4861 Å for 3C 184.1 and 35% for Mrk 198. Evidence for young and intermediate-age stars in the spectra of Mrk266SW was reported by Wang et al. (1997). According to Gonçalves, Véron-Cetty, & Véron (1999), this galaxy also has a composite emission line spectrum, with emission line ratios intermediate between those of Seyferts and starbursts. The same description is given for the interacting galaxy NGC 4922B by Alonso-Herrero et al. (1999). We could not find information regarding the compositeness or otherwise of the remaining galaxies. Our prediction is that most of them should present detectable signatures of circumnuclear starburst activity.

3.3.2. *Moderate and Weak FC Sources Are Ambiguous*

While all $x_{FC} \gtrsim 30\%$ sources are composites, *the converse is not true.* For IC 3639, a galaxy whose composite nature has been conclusively established by both optical and UV spectroscopy, we find a 16% FC. The range between 15% and 30% also contains four "pure" Seyfert 2 nuclei: NGC 1068, Mrk 3, NGC 7212, and Mrk 34.

NGC 1068 is sometimes listed as an example of a starburst-AGN link because of its bright ring of H II regions at ~ 1 kpc from the nucleus, which contributes roughly half of the bolometric (IR) luminosity of this prototype Seyfert 2 (Telesco et al. 1984; Lester et al. 1987). If observed from further away, the ring would dominate the optical spectrum, imprinting signatures which would cast distant NGC 1068's in the composite category (Heckman et al. 1995; Colina et al. 1997), but, as argued in § 2, this is not the effect behind the starburst features identified in our composites (Fig. 1). The spectrum of NGC 1068 analyzed here pertains to a much smaller region, corresponding to $r_{ap} = 66$ pc. The only indications of star formation within this central region are the strong Ca II triplet at ~ 8500 Å (Terlevich, Díaz, & Terlevich 1990) and the small M/L ratio at 1.6 μm (Oliva et al. 1995, 1999), both of which point to an intermediate-age population, qualitatively consistent with the $x_{INT} = 11\%$ found in our synthesis. There does not seem to be substantial ongoing star formation associated with this "poststarburst" population, since neither far-UV (Caganof et al. 1991) nor optical (GD01; Miller & Antonucci 1983) spectroscopy reveal signs of young stars close to the nucleus. Furthermore, from the work of Antonucci & Miller (1985), Miller & Goodrich (1990), and Tran (1995c) we know that NGC 1068 does *not* suffer from the "FC2 syndrome" (lower polarization in the continuum than in the broad lines), so most, if not all, of its nuclear FC is indeed FC1. Since our x_{FC} estimate is in fair agreement with previous determinations (e.g., the 22% at 4600 Å found by Miller & Antonucci 1983 and the 16% at 5500 Å derived by Tran 1995c), there is little doubt that $x_{FC1} \gg x_{YS}$ in the central region of NGC 1068. We therefore keep NGC 1068 in the "pure" Seyfert 2 category.

The nature of the FC is not so clear for the 3 other moderate FC "pure" Seyfert 2's in our sample: Mrk 3, NGC 7212, and Mrk 34. In their detailed analysis of the same data used here, GD01 find that the dilution of the metal absorption lines in these galaxies is better modeled by an elliptical galaxy plus power-law spectral decomposition than using an off-nuclear template, which, together with the lack of starburst features, lead them to favor a scattered light origin for their FC. The extended blue continuum aligned with the radio axis and ionization cone in Mrk 3 (Pogge & De Robertis 1993) supports this idea. Kotilainen & Ward (1997) find a similar feature in NGC 7212, though not aligned along the [O III] emission. These indications of a FC1 component are confirmed by the spectropolarimetry observations of Tran (1995a, 1995b, 1995c), which revealed their hidden Seyfert 1 nuclei. However, Tran also finds that Mrk 3 and NGC 7212 suffer from acute "FC2-itis"! According to his analysis, only 4% (Mrk 3) and 2% (NGC 7212) of the flux at 5500 Å is attributable to FC1; the rest of their FC is "FC2"! The total FC = FC1 + FC2 fractions at 5500 Å found by Tran are 12% for Mrk 3 and 17% for NGC 7212, which are in very good agreement with our estimates of x_{FC} when translated to the same wavelength. Therefore, from the point of view of their polarization spectra, most of their FC still have to be explained.

Below $x_{FC} \sim 30\%$ we therefore enter a "gray zone": the power-law/starburst degeneracy sets in and the identity of the FC becomes ambiguous. Extra information (spectropolarimetry, UV spectroscopy, imaging) may help disentangling these two components in a few sources, but the situation becomes even fuzzier for weak FC sources ($x_{FC} < 15\%$). The case of Mrk 348 is illustrative in this respect. Using an elliptical galaxy template, Tran (1995a, 1995b) finds a 27% FC at 5500 Å, which, when combined with his spectropolarimetry data, propagates to the conclusion that 22% of the total light is associated with something else, i.e., FC2. Storchi-Bergmann et al. (1998), on the other hand, find a much weaker FC by using an off-nuclear spectrum as a starlight template, a conclusion corroborated by GD01 on the basis of independent observations. In fact, they find that the nuclear spectrum is well matched with no FC at all, but, guided by the results of Tran, they favor a model in which 5% of the light comes from the FC1 component detected via spectropolarimetry.

These inconsistencies undoubtedly emerge due to the intrinsic weakness of the FC, which, combined with the dispersion of stellar populations in active galaxies (Cid Fernandes et al. 1998; Schmitt et al. 1999; Boisson et al. 2000; GD01), boosts the differences between different FC estimation methods. Whereas in Mrk 348 the combination of spectropolarimetry and long-slit spectra allowed considerations about the nature of its FC, we do not have such information for most sources below Mrk 348 in Table 3, and even if such data existed, it is clear that any attempt to perform a detailed spectral decomposition would be highly uncertain, since it is simply unrealistic to expect accuracies better than $\sim \pm 5\%$ in any x_{FC} determination method. From the point of view of this paper, we consider all such

sources ambiguous. We hope to shed light on the nature of these moderate and weak FC Seyfert 2's by considering information other than that contained in the optical continuum and absorption lines (§ 4).

3.4. *Empirical Calibration of the FC Strength*

As in any other study dealing with optical spectra of Seyfert 2's, the FC strength plays a major role throughout this paper. The results above already indicate that, regardless of the ambiguities involved in the interpretation of $x_{\rm FC}$, our method was able to recover a meaningful component of the near-UV–optical continuum, a conclusion which will become stronger in the analysis that follows. This in itself is an important result, since we based our FC estimation on just a handful of easily measurable quantities. Though the synthesis process is rather elaborate, we may use its results to derive an a posteriori calibration of $x_{\rm FC}$ in terms of the observables it is based upon. In fact, as shown in Figure 3, we find that the expression

$$x_{\rm FC} = -0.33\left(\frac{W_{\rm K}}{20}\right) + 0.52\left(\frac{W_{\rm K}}{20}\right)^2 + 0.89\left(\frac{F_{3660}}{F_{4020}}\right) - 1.04\left(\frac{W_{\rm K}}{20}\right)\left(\frac{F_{3660}}{F_{4020}}\right) - 0.08\ , \quad (1)$$

where $W_{\rm K}$ is in Å, recovers $x_{\rm FC}$ within $\pm 3\%$ for all galaxies. Since the measurements of both $W_{\rm K}$ and the F_{3660}/F_{4020} color do not require large S/N spectra, this calibration can be applied to data sets not meeting the S/N > 25 standard of our sample (which was necessary to identify weak starburst features). This provides a much more straightforward and well-defined way to estimate $x_{\rm FC}$.

Although old stars are of no direct interest in the starburst-AGN connection, we have seen that they play a central role in defining the detectability of circumnuclear starbursts, so it is useful to have an equation analogous to equation (1) for $x_{\rm OLD}$. We find that

$$x_{\rm OLD} = 1.92\left(\frac{W_{\rm K}}{20}\right) - 0.98\left(\frac{W_{\rm K}}{20}\right)^2 + 0.05 \quad (2)$$

reproduces the synthetic $x_{\rm OLD}$ to better than $\pm 5\%$ for all galaxies.

Equations (1) and (2) also do a good job for the merger, NLAGN, and Starburst samples. This is illustrated in Figure 3*b* for the galaxies in the Starburst sample. The difference, of course, is that for these bona fide starbursts the FC is undoubtedly produced by young stars.

A corollary of $x_{\rm FC}$ and $x_{\rm OLD}$ being so closely related to $W_{\rm K}$ is that this quantity can be used as a first order measure of the stellar population mix and the spectral dilution of metallic features of old stars caused by young stars, a power-law or a combination of both. Indeed, in several of the plots below $W_{\rm K}$ is used with this function, since, for most practical purposes, $W_{\rm K}$ and $x_{\rm FC}$ are equivalent (Fig. 3).

4. EMISSION LINES

Circumnuclear starbursts in Seyfert 2's act as a second source of ionizing photons besides the hidden AGNs, and as such are bound to contribute at some level to their emission line spectrum. In this section we examine our sample in search of signs of this contribution, analyzing the equivalent widths of strong emission lines (§ 4.1), emission line ratios (§ 4.3), and line profiles (§ 4.4). An investigation of line-FC relations is also presented (§§ 4.2 and 4.5). When referring to emission line equivalent widths measured with respect to the FC we will use the notation $W_\lambda^{\rm FC} \equiv W_\lambda^{\rm obs}/x_{\rm FC}$ to distinguish them from the observed ones, denoted by $W_\lambda^{\rm obs}$.

4.1. *The Equivalent Widths of* Hβ, [O III] *and* [O II]

The effect of a circumnuclear starburst on the $W_{\rm H\beta}^{\rm FC}$ of Seyfert 2's is easily predicted by considering the inverse situation: a pure starburst to which we add a Seyfert 2. The

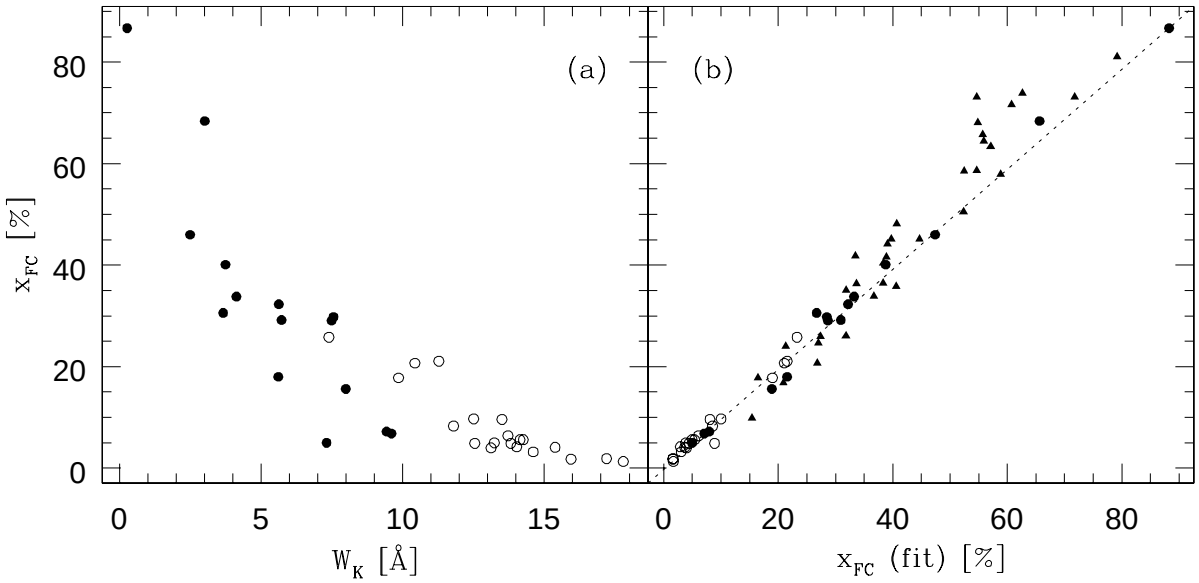

FIG. 3.—(*a*) Relation between the FC strength at 4861 Å and the equivalent width of Ca II K for the Seyfert 2 sample. Composites are plotted with filled circles. (*b*) Comparison of the FC strengths derived from the synthesis and from the empirical fit of $x_{\rm FC}$ as a function of $W_{\rm K}$ and a near-UV color (eq. [1]), which offers an easy way of estimating $x_{\rm FC}$. Starburst galaxies from the SBMQ95 data are also included in this plot (*filled triangles*), but not in the fit.

latter will surely add more to the Hβ flux than to its underlying continuum, since the nonstellar FC from the active nucleus is only seen periscopically and hence strongly suppressed in the scattering process, whereas photons from the narrow line region (NLR) do not suffer such suppression because they are not obscured by the pc scale dusty torus which surrounds the nucleus. The net effect of this superposition is that Seyfert 2's should have a larger ratio of line per FC photons than in pure starbursts.

This expectation is totally confirmed in the left panels of Figure 4, where we compare the distribution of $W^{\rm FC}_{\rm H\beta}$ for our Seyfert 2 sample with that of the 35 starburst galaxies in the starburst sample. *These histograms reveal a clear offset in $W^{\rm FC}_{\rm H\beta}$ between Seyfert 2's and stellar powered emission line sources.* The median $W^{\rm FC}_{\rm H\beta}$ is a factor of 5 larger in the Seyfert 2 sample than in pure starbursts (129 compared to 26 Å).

Given their dual nature, we intuitively expect composite systems to exhibit $W^{\rm FC}_{\rm H\beta}$ in between those of "pure" Seyfert 2's and starbursts. This expectation is also confirmed. The composite Seyfert 2/starburst systems in our sample, marked by the filled region in Figure 4*a*, tend to populate the low end of the $W^{\rm FC}_{\rm H\beta}$ distribution in Seyfert 2's, overlapping with the high $W^{\rm FC}_{\rm H\beta}$ starbursts (Fig. 4*b*).

The same considerations, of course, apply to other emission lines. In fact, given that [O III]/Hβ is much larger in Seyferts than in stellar powered systems, we expect an even clearer separation between these two types of objects in terms of $W^{\rm FC}_{\rm [O\,III]}$. This is confirmed in Figures 4*c* and 4*d*. The difference between median $W^{\rm FC}$-values, which was a factor of 5 for Hβ, is now 32-fold, with 44 Å for Starburst galaxies and 1431 Å in the Seyfert 2 sample. As for Hβ, composites are skewed toward low $W^{\rm FC}_{\rm [O\,III]}$-values (Fig. 4*c*). The same effects are identified in [O II] (Figs. 4*e* and 4*f*).

The large offset in $W^{\rm FC}$-values between Seyfert 2's and Starburst galaxies is not an artifact of aperture differences between the two samples. One does not expect drastic changes in the line per continuum photon ratio between nuclear and off-nuclear star-forming regions, so the distribution of $W^{\rm FC}$-values for Starburst galaxies should remain roughly the same for small and large apertures. This is demonstrated by the shaded portions of the histograms in Figures 4*b*, 4*d*, and 4*f*, which mark Starburst galaxies observed through physical apertures $r_{\rm ap} < 1$ kpc. Aperture effects become important for Seyfert 2's, since there the contribution of off-nuclear H II regions affects the line/FC proportion, diluting the higher $W^{\rm FC}$ of the nucleus. This effect is detected for the objects in common between the Seyfert 2 and NLAGN samples. Mrk 477, for instance, has $W^{\rm FC}_{\rm H\beta} = W^{\rm obs}_{\rm H\beta}/x_{\rm FC} = 35/0.47 = 75$ Å for the observations of SBMQ95, whereas with our nuclear spectra we obtain 92/0.87 = 107 Å. The same effect occurs comparing the nuclear with the "whole aperture" spectra of LK95, which integrate over the entire galaxy.

Since in § 3 we found that composites tend to have a strong FC, we may expect them to be well separated from "pure" Seyfert 2's in diagrams involving $x_{\rm FC}$ and these emission line $W^{\rm FC}$-values. This is illustrated in Figures 5*a*–5*c*, where we plot the $W^{\rm FC}$-values of Hβ, [O III] and [O II] against $W_{\rm K}$, here representing the FC strength. Note that all composites are located to the left of the $W_{\rm K} = 10$ Å line indicated in the plots. (A slightly more stringent constraint of $W_{\rm K} < 8.5$ Å can be adopted by restraining our

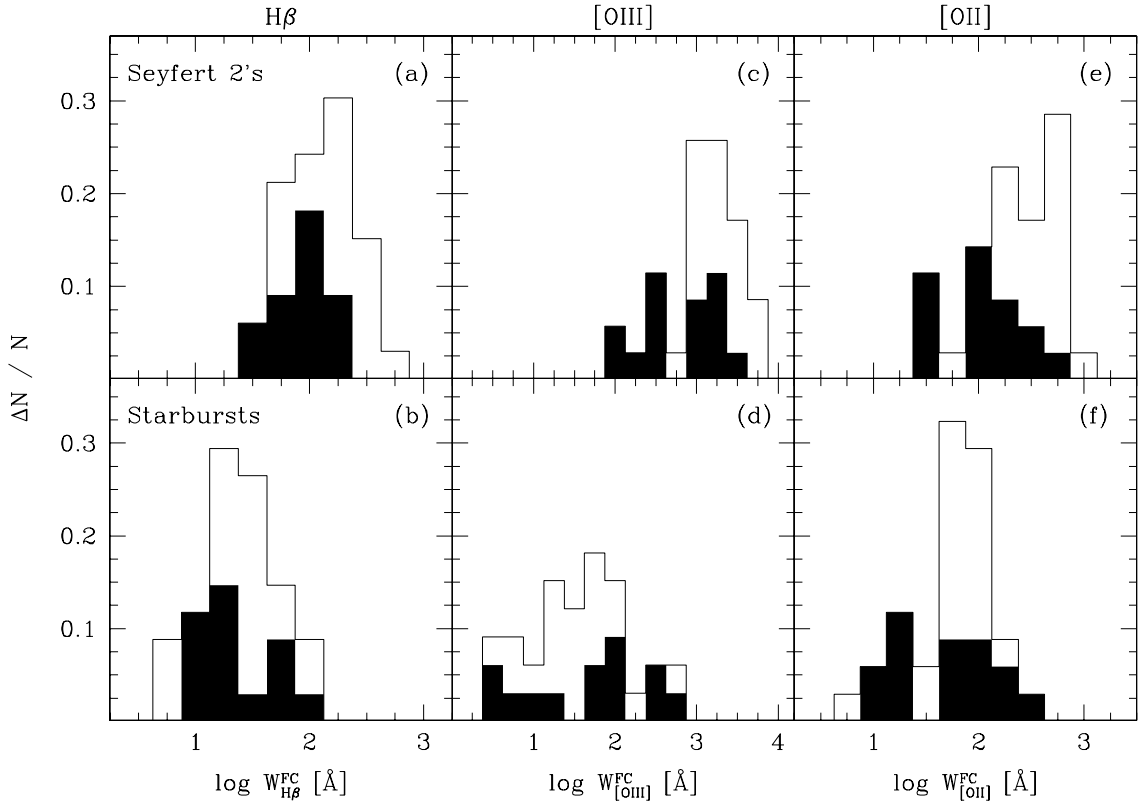

FIG. 4.—*Top*: Distribution of the equivalent widths of Hβ, [O III] and [O II] for the sources in the Seyfert 2 sample. The shaded regions indicate the composites only. *Bottom*: As above for galaxies in the Starburst sample. The shaded histogram marks galaxies observed through $r_{\rm ap} < 1$ kpc apertures. All W-values are measured with respect to the featureless continuum, whose strength $x_{\rm FC}$ was estimated from our synthesis analysis. In the Hβ and [O III] plots the FC strength is evaluated at 4861 Å, whereas for [O II] we evaluate $x_{\rm FC}$ at 3660 Å.

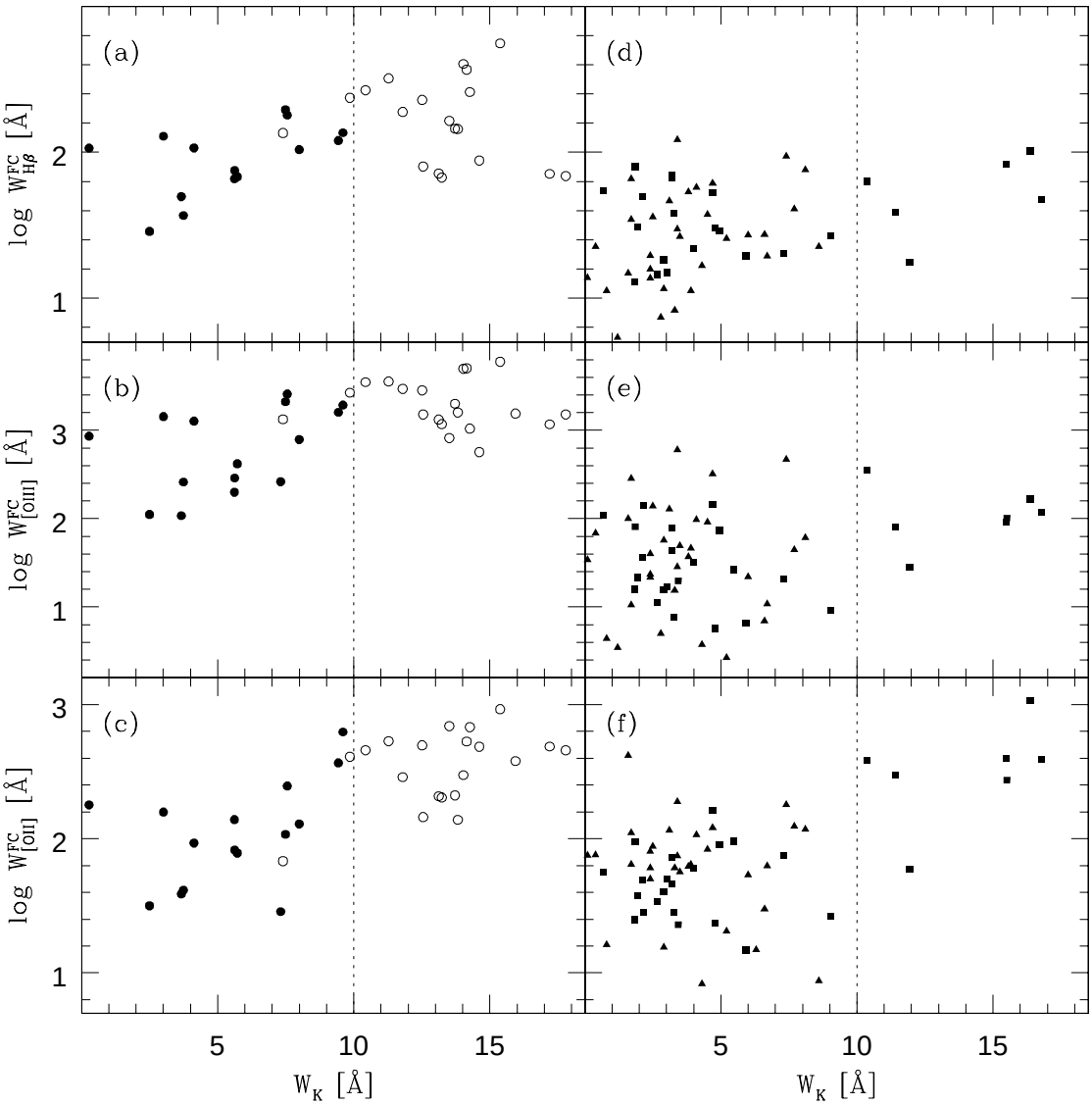

FIG. 5.—Equivalent widths of Hβ (*top*), [O III] (*middle*) and [O II] (*bottom*) with respect to the FC against W_K. Sources from the Seyfert 2 sample are in the left (*a–c*), whereas plots in the right (*d–f*) show the Starburst and merger samples. Symbols follow the same convention as in Fig. 2. The location of Seyfert 2's in the $W_K \times W^{FC}_{H\beta}$ diagram (*a*) can be used to assess the *degree of difficulty is identifying starburst features*: Sources to the lower left (weak W_K and $W^{FC}_{H\beta}$) have a strong, starburst-dominated FC, whereas we do not know with certainty what dominates the weak FC sources in the top right of the diagram.

definition of composites to systems which exhibit signs of young stars, thus excluding the poststarbursts NGC 5643, Mrk 78, and ESO 362-G8.) The W^{FC}-values by themselves do not segregate composite from "pure" Seyfert 2's as efficiently as W_K, but sources with the weakest emission lines are predominantly composites, so the vertical axis provides some extra diagnostic power. The "pure" Seyfert 2 at $W_K = 7.4$ Å, trespassing the $W_K < 10$ Å zone of composites, is NGC 1068, which has $W^{FC}_{[O\,II]} = 68$, $W^{FC}_{[O\,III]} = 1334$ and $W^{FC}_{H\beta} = 136$ Å. This prototype Seyfert 2, which shows no optical-UV signs of recent star formation close to the nucleus, is located either among or close to the composites in all diagrams presented in this paper. We will return to this issue in § 7. The panels on the right side of Figure 5 show the results for sources in the starburst and merger samples for comparison.

4.1.1. *The Difficulty in Identifying Circumnuclear Starbursts*

Once again we must draw attention to contrast effects which may lead us to classify Seyfert 2's with weak circumnuclear starbursts as "pure" systems. Part of the difficulty in identifying starburst features in Seyfert 2 nuclei with strong emission lines comes from the fact that as $W^{FC}_{H\beta}$ increases the high-order H I Balmer absorption lines of massive stars become increasingly filled up by emission. In the absence of far-UV spectra (available for very few sources) and the short-lived WR bump, this effect effectively prevents us from seeing the starburst in the near-UV to optical range.

This contrast effect comes on top of the difficulty in identifying circumnuclear starbursts in systems dominated by the old stellar population (§ 3.2). The combination of these two effects may be at least partly responsible for the horizontal and vertical separations between composites and "pure" Seyfert 2's seen in Figures 5*a*–5*c*. The location of a Seyfert 2 in the W_K-$W^{FC}_{H\beta}$ plane can therefore be read as an empirical measure of the "*degree of difficulty*" in the recognition of circumnuclear starbursts in Seyfert 2's: Sources at the bottom left are easily identified as composites, whereas as one progresses to the top right it becomes

increasingly difficult to discern the starburst features. The usefulness of this concept is illustrated by the location of Mrk 3, Mrk 34, and NGC 7212 in Figures 5*a*–5*c*: all are around the $W_K = 10$ Å "dividing line" but with $W^{FC}_{H\beta}$ and $W^{FC}_{[O\,III]}$ larger than for composites. It is no accident, therefore, that the nature of their moderately strong FC remains unclear (§ 3.3.2).

4.2. *The Relation between Line and FC Emission*

It is important to emphasize that the offset in emission line equivalent widths between Seyfert 2's and starbursts only appears when these are measured with respect to the FC, as hinted in Figure 5. Our estimate of x_{FC}, which takes into consideration continuum colors and metal absorption lines through our semiempirical synthesis analysis, is thus the key behind this significant offset.

The role of the synthesis process can be better appreciated in Figure 6. In Figure 6*a* we plot $F_{H\beta}$ against the total observed continuum flux at 4861 Å. What is seen is a scatter diagram, which is not surprising since the continuum in most sources is dominated by old stars and thus has little relation to the line emission. This is confirmed by the fact that the scatter increases even further if the continuum fluxes are multiplied by x_{OLD} (Fig. 6*b*), thus isolating the flux due to ≥ 1 Gyr stars. The line versus continuum plot changes dramatically when we isolate the FC contribution! Using $F_{FC} = F^{obs}_{4861} \times x_{FC}$ in the abscissa (Fig. 6*c*) has the remarkable effect of uncovering an underlying order immersed in the scatter plot on the left. It is therefore clear that *our FC determination method isolated a component of the optical continuum which is directly linked to the line emission*, lending further credibility to the inferred x_{FC}-values. The same result is obtained for the sources in our comparison samples, i.e., x_{FC} organizes the data along a $F_{H\beta}$-F_{FC} correlation which is not evident in the $F_{H\beta}$-F^{obs}_{4861} plane because of the contribution of the old stellar population.

Possible interpretations of the Hβ-FC relation identified in Figure 6*c* will be discussed in § 4.5, after we gather other related results. To substantiate the discussion it is useful to compare it to the equivalent relation in starburst systems and to investigate line-FC relations for other transitions. This is done in Figures 7 and 8, which contain luminosity-luminosity versions of Figure 6*c* for the Seyfert 2, Starburst, and NLAGN samples and for Hβ, [O II], [O III] and He II. Lines of constant $W^{FC} = 10$, 100, and 1000 Å run diagonally across these plots to facilitate their intercomparison. Also to aid the discussion, Table 4 summarizes the results of a Spearman rank correlation analysis for flux-flux line-continuum relations. The values listed are the probabilities of chance correlation (p_S), so small values indicate significant correlations.

Significant line-FC correlations are also obtained for [O II], [O III] and He II in the Seyfert 2 sample (Figs. 7*c*, 8*a*, and 8*c*, Table 4). Note, however, that the scatter in the [O III] and He II plots is visibly larger than for Hβ-FC (Fig. 7*a*). It is also clear that a substantial part of the scatter in these plots is induced by the offset location of the composites toward smaller W^{FC}-values. Statistical confirmation of this effect is provided in Table 4, where these correlations are examined for the whole sample and for subsets containing only "pure" or composite systems.

Starburst galaxies also follow a tight Hβ-FC relation, with $W^{FC}_{H\beta} = 10$–100 Å (Fig. 7*b*, *filled triangles*). This is a long known (Terlevich et al. 1991) and well-understood behavior of stellar powered systems, for which F_{FC} actually represents the contribution of young stars and hence traces the ionizing flux. Current models (e.g., Leitherer et al. 1999) predict $W_{H\beta}$ between 400 and 10 Å for constant star formation, different IMFs and ages up to 10^8 yr. These are broadly consistent with the values we obtain, but a detailed comparison with such evolutionary models will have to await a cross-calibration of our semiempirical synthesis decomposition in terms of the theoretical spectra. As for the Seyfert 2 sample, the second best line-FC relation for starburst galaxies is that with the [O II] line (Fig. 7*d*). This too is a well-known relation, which has in fact been used as an alternative estimator of star formation rates in galaxies (Gallagher et al. 1989; Kennicutt 1992; Tresse et al. 1999; Jansen, Franx, & Fabricant 2001).

The location of the NLAGNs in these plots (*open triangles*) reflects the mixed nature of this sample. Some of them behave just like "pure" Seyfert 2's, most notably

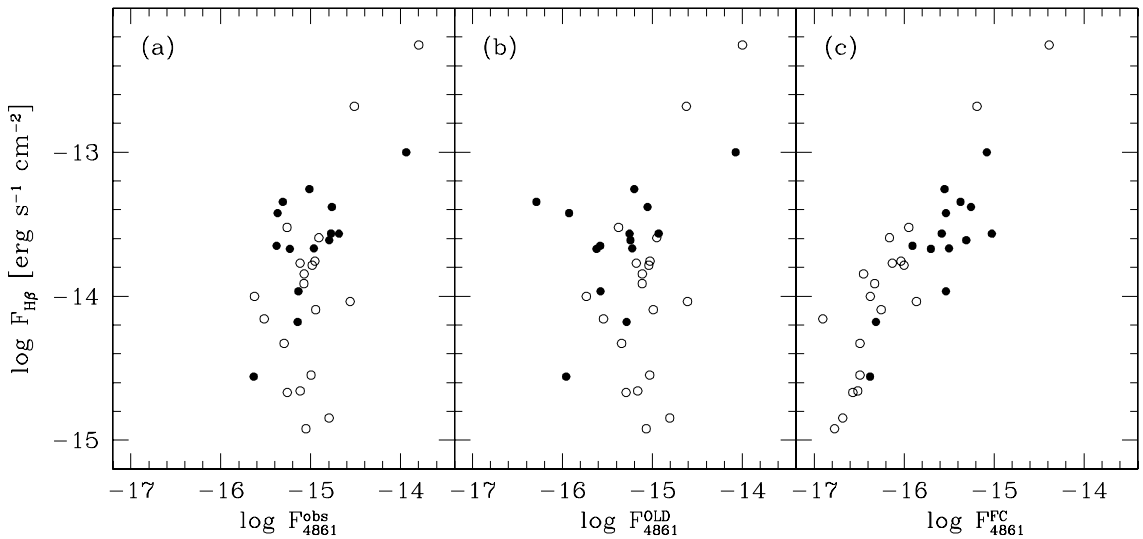

FIG. 6.—Relation between the continuum at 4861 Å and Hβ fluxes. The panels differ in which component of F_{4861} is used in the abscissa. (*a*) Total observed continuum. (*b*) $F_{4861} \times x_{OLD}$, i.e., the continuum flux due to old stars. (*c*) $F_{4861} \times x_{FC}$, the FC flux. Symbols as in Fig. 2. All continuum fluxes are given in ergs s^{-1} cm^{-2} Å^{-1}. Notice how x_{FC} has the property of unveiling a strong line-continuum correlation immersed in the scatter plot on the left.

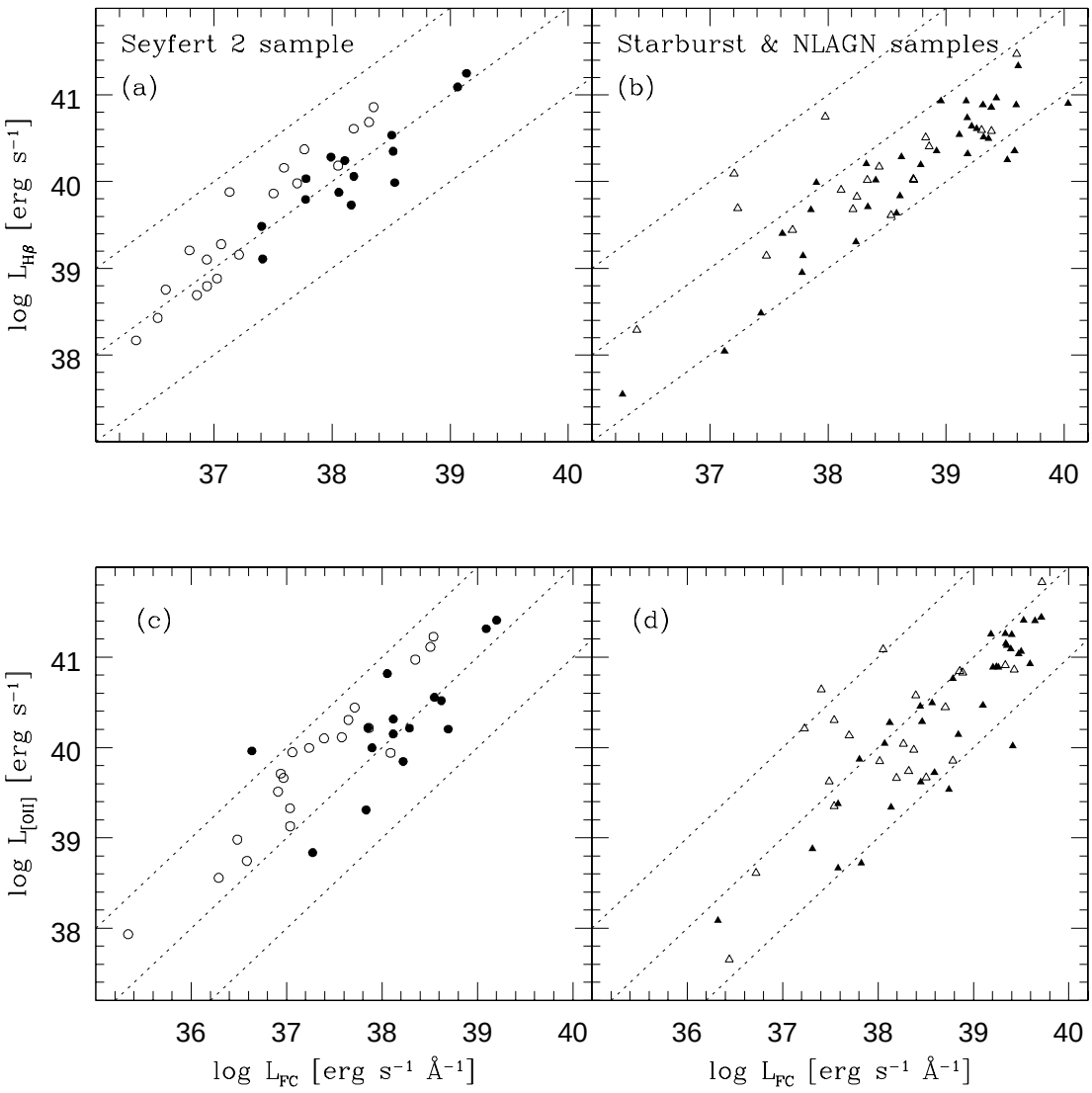

FIG. 7.—Relation between the Hβ (*top*) and [O II] (*bottom*) luminosities and the FC luminosity $L_{FC} = L_{obs} \times x_{FC}$ for the Seyfert 2 (*left*), Starburst, and NLAGN samples (*right*). Note that L_{FC} is evaluated at 4861 Å for the Hβ plot and at 3660 Å for [O II]. Diagonal lines indicate, from bottom to top, $W^{FC} = 10$, 100, and 1000 Å. Symbols as in Fig. 2.

NGC 3393 and NGC 5506, which stand out in Figures 7*b*, 7*d*, and 8*b* as the sources with highest W^{FC}-values. Most of the other NLAGNs are mixed among Starburst galaxies in these plots. This happens due to a combination of the aperture effects discussed in § 4.1 and the fact that this sample contains several composites and some objects which are more consistent with a LINER classification (e.g., NGC 1097, NGC 1433). It is thus clear that these galaxies do not constitute a well-defined comparison sample. For these reasons, we concentrate on the comparison between the Seyfert 2 and Starburst samples.

4.2.1. *Extinction*

One would like to believe that extinction does not play a relevant role in these line-FC diagrams since both axes correspond to similar wavelengths. In Starburst galaxies, however, it is known that the continuum suffers $\sim$2 times less extinction than the emission line region (Calzetti, Kinney, & Storchi-Bergmann 1994). This effect can reshuffle the data points in the plots above, potentially changing the overall appearance and strength of the line-FC correlations.

An estimate of the effects of extinction is presented in Figure 9 for the Hβ-FC relation using the Hα/Hβ-values listed in Table 2. Figure 9*a* presents the data with L_{FC} and $L_{H\beta}$ dereddened by the same amount, whereas in Figure 9*b* we halved the optical depth to the FC. Two effects are clear when comparing these plots with their uncorrected counterpart (Fig. 7*a*): First, with the extinction correction, composites are more segregated from "pure" Seyfert 2's in terms of $L_{H\beta}$, with median values which differ by an order of magnitude (median $L_{H\beta} = 1.6 \times 10^{41}$ and 1.7×10^{40} ergs s^{-1} for composites and "pure" Seyfert 2's, respectively). This preference of composites for luminous systems will appear again when we discuss their far-IR luminosities in § 5. Second, a differential line/FC extinction correction only tightens the Hβ-FC correlation! The effect is such that it practically erases the offset in $W^{FC}_{H\beta}$ between composite and "pure" Seyfert 2's.

The caveats in these results are that the Hα/Hβ-values used were not obtained from the same spectra we analyze (§ 2) and that we do not know whether the $\tau_{FC} \sim \tau_{H\beta}/2$ result applies to AGNs. At any rate, the larger Hα/Hβ of compos-

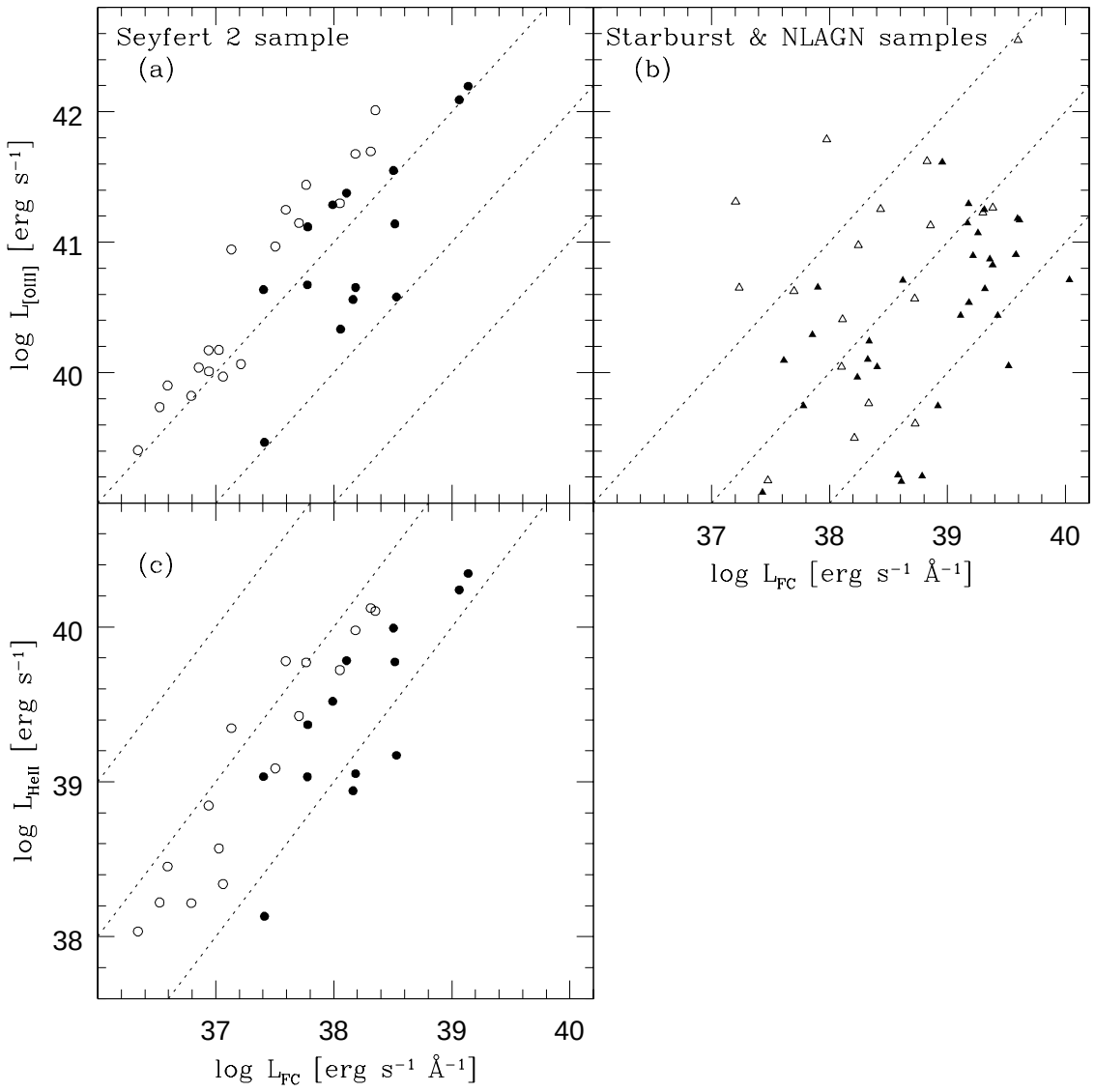

FIG. 8.—Same as Fig. 7, but for the [O III] and He II emission lines. No He II measurements are available for the Starburst and NLAGN samples.

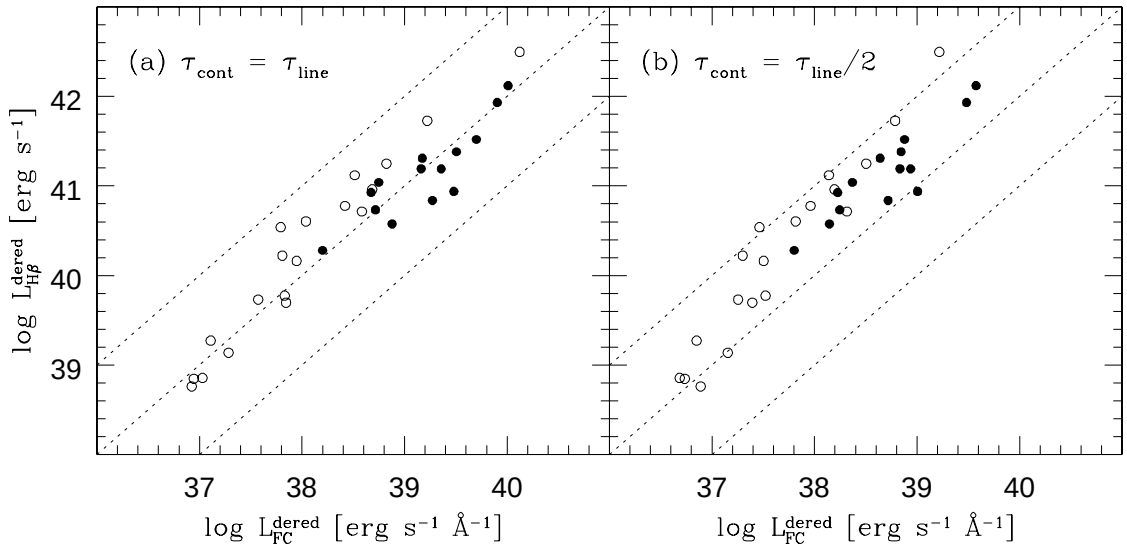

FIG. 9.—(*a*) Dereddened FC vs. Hβ relation for the Seyfert 2 sample after correcting both axis for the extinction implied by Hα/Hβ. (*b*) As above, but assuming the continuum is only half as extincted as the emission lines (Calzetti et al. 1994). Symbols and lines as in Fig. 7.

TABLE 4

LINE-FC CORRELATIONS

	WHOLE SAMPLE				COMPOSITES				"PURE" SEYFERT 2'S			
FLUX	F_{obs}	F_{OLD}	F_{SB}	F_{FC}	F_{obs}	F_{OLD}	F_{SB}	F_{FC}	F_{obs}	F_{OLD}	F_{SB}	F_{FC}
$F_{H\beta}$	7×10^{-2}	7×10^{-1}	2×10^{-7}	6×10^{-11}	5×10^{-1}	6×10^{-1}	3×10^{-1}	2×10^{-2}	2×10^{-1}	3×10^{-1}	9×10^{-5}	2×10^{-6}
F_{HeII}	3×10^{-2}	9×10^{-2}	5×10^{-3}	2×10^{-3}	-9×10^{-1}	7×10^{-1}	-6×10^{-1}	-5×10^{-1}	1×10^{-2}	2×10^{-2}	1×10^{-3}	7×10^{-4}
$F_{[OIII]}$	2×10^{-1}	5×10^{-1}	1×10^{-3}	4×10^{-5}	-8×10^{-1}	9×10^{-1}	-6×10^{-1}	9×10^{-1}	2×10^{-1}	3×10^{-1}	5×10^{-4}	3×10^{-5}
$F_{[OII]}$	1×10^{-3}	1×10^{-1}	1×10^{-4}	2×10^{-6}	3×10^{-1}	8×10^{-1}	5×10^{-1}	3×10^{-2}	3×10^{-3}	2×10^{-2}	3×10^{-5}	3×10^{-5}
F_{FIR}	4×10^{-2}	7×10^{-1}	3×10^{-5}	1×10^{-4}	9×10^{-2}	3×10^{-1}	4×10^{-2}	5×10^{-1}	2×10^{-1}	3×10^{-1}	5×10^{-2}	5×10^{-3}

NOTES.—Probability p_S of chance flux-flux correlation in a Spearmann rank test (the smaller p_S the better the correlation). Negative probabilities denote anticorrelations. F_{obs} denotes the total optical continuum at 4861 Å (3660 Å for the correlation with [O II]). F_{OLD}, F_{SB}, and F_{FC} are the fluxes associated with the x_{OLD}, $x_{INT} + x_{FC}$, and x_{FC} fractions, respectively.

ites, which is responsible for this regrouping, is consistent with UV (Heckman et al. 1995) and X-ray (Levenson, Heckman, & Weaver 2001b) indications that circumnuclear starbursts in Seyfert 2's are substantially reddened and may significantly contribute to the extinction of the AGN component in such composite systems. This "excess" of dust is probably associated with the same gas which feeds the starburst activity, but more work will be required to address this issue quantitatively.

4.3. *Do Starbursts Participate in the Ionization of the Gas in Seyfert 2 Galaxies?*

The results reported so far show how the presence of circumnuclear starbursts manifests itself in the FC strength and the equivalent widths of emission lines. These results per se do not necessarily imply that the starburst contributes to the ionization of the line emitting gas in Seyfert 2's, since it may act mostly as a source of FC, diluting an AGN powered Hβ emission and thus shifting points to the right, but not much upward in Figures 6–9. One way to establish whether the starburst participates in the ionization of the gas is to investigate the ratio between He II λ4686 and Hβ. Unlike AGNs, starbursts do not produce significant radiation above 54 eV, so they show little He II emission. If starbursts in AGNs contribute to Hβ this ratio will tend to be smaller in composites than in "pure" Seyfert 2's.

This is confirmed in Figures 10*a* and 10*b*, where we plot He II/Hβ against W_K and x_{OLD}, both empirical indicators of compositeness (§ 3). Whereas the whole sample spans the 0.1–0.8 interval in He II/Hβ, all composites have He II/Hβ < 0.4. Many "pure" Seyfert 2's also have He II this weak, but their stronger Ca II K and hence larger x_{OLD} clearly separates them from composites. Starburst galaxies would be located in the same horizontal range spanned by composites in Figures 10*a*–10*b*, but down to weaker He II (a line which is often not detected in starbursts). Composites also tend to be less excited in terms of [O III]/Hβ, as shown in Figures 10*c*–10*d*. The effect of the stellar absorption feature underneath the Hβ emission-line was not corrected for in this analysis. Since composites are more likely to have stronger Balmer absorption lines than objects dominated by old stars, this correction would only strengthen our conclusion, shifting the composites to even smaller He II/Hβ and [O III]/Hβ ratios.

Either line ratio can therefore be used as an auxiliary diagnostic of compositeness. This is illustrated by the dotted lines in Figure 10, which isolate composites from "pure" Seyfert 2's almost completely! (Again, the oddball is NGC 1068.) This shows a welcome consistency between diagnostics of compositeness based on continuum and stellar features and the expected impact of circumnuclear starbursts upon the emission line ratios in Seyfert 2's. Note, however, that while all known composites have low excitation, the converse is not true, since many "pure" Seyfert 2's lie in the He II/Hβ < 0.4 and [O III]/Hβ < 15 range defined by composites. In terms of emission line ratios, these galaxies could well have circumnuclear starbursts, but which do not make it to the composite class due to the contrast effect discussed above.

It is hard to see how to account for these results in a "pure AGN" scenario. The shape of the ionizing spectrum, the proportion of matter to ionization-bounded clouds and

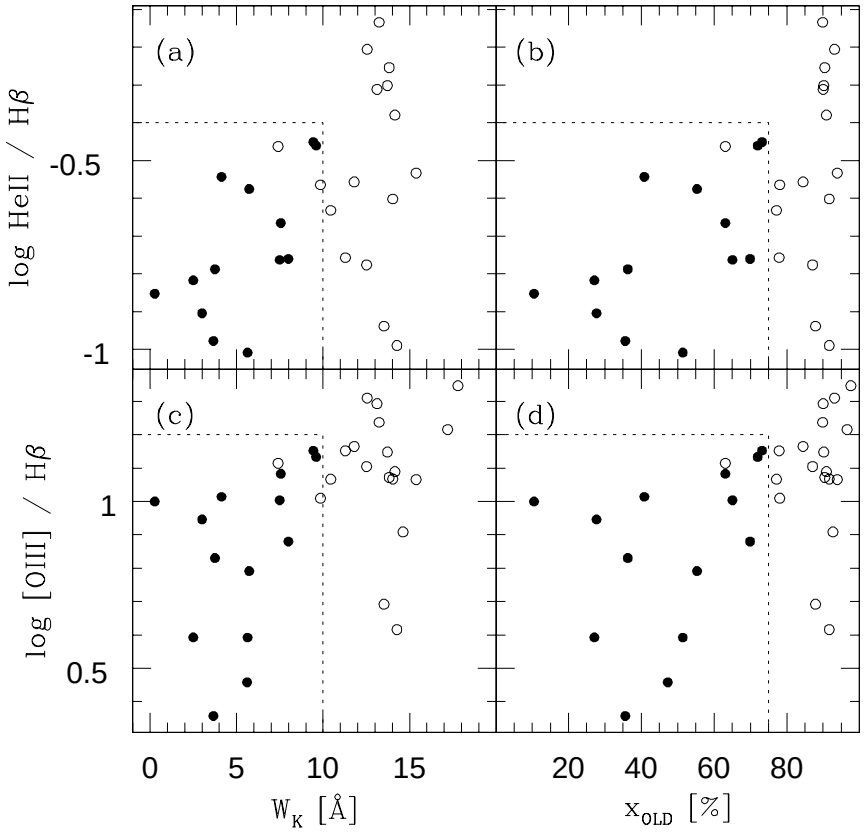

FIG. 10.—"Excitation" ratios plotted against indicators of circumnuclear starbursts for the Seyfert 2 sample. Filled circles mark composite systems and open circles mark "pure" Seyfert 2's. Dotted lines delimit regions occupied by composites and may be used as empirical diagnostics of compositeness.

the ionization parameter are just some of the factors which define the excitation level of the NLR, and source-to-source variations of these properties can account for a wide spread in He II/Hβ and [O III]/Hβ (e.g., Viegas-Aldrovandi 1988). Yet, none of these intrinsic properties explains the "zone of avoidance" for strong FC and high excitation in Figure 10. If anything, a strong FC would suggest a higher ionization parameter and perhaps a harder ionizing spectrum, which would produce higher excitation, contrary to what is observed. Overall, the simplest interpretation of these data is that part of the emission lines in composites originates from photoionization by a circumnuclear starburst. This contribution is strongest in Hβ, since starbursts are inefficient producers of He II and [O III] compared to AGNs.

It is clear that in a starburst + AGN mixture of emission lines the starburst component can dominate Hβ without moving the source outside of the AGN region in diagnostic diagrams (e.g., Hill et al. 2001; Levenson et al. 2001a). For instance, using typical [O III]/Hβ ratios of 10–20 for Seyfert 2's and 0.3–1 for metal-rich starbursts, the total ratio still lies within the [O III]/H$\beta > 3$ domain of Seyferts for as much as 70%–90% of Hβ powered by the starburst! Therefore, our conclusion that photoionization by massive stars provides a substantial part of $L_{\rm H\beta}$ in composites is not in conflict with their Seyfert 2 classification. In fact, this conclusion was already implicit in the offset in $W_{\rm H\beta}^{\rm FC}$ between composites and Starburst galaxies (Fig. 4). The $W_{\rm H\beta}^{\rm FC}$-values in composites cover the range from 30 to 200 Å, which may be represented by its geometric mean of $\sim$80 Å. The corresponding value in Starburst galaxies is $\sim$30 Å, representing the $W_{\rm H\beta}^{\rm FC} = 10$–100 Å interval. Since we know that the FC in composites is dominated by the starburst component, these values imply a typical starburst contribution of 30/80 $\sim$ 40% to Hβ.

These results imply that Hβ is partially powered by the starburst in composite systems. Unfortunately, as for $L_{\rm FC}$, it is not possible to unambiguously separate the starburst and AGN shares of $L_{\rm H\beta}$ without extra information, such as assuming typical line ratios or equivalent widths. For instance, taking the mean [O III]/Hβ of 13 for our "pure" Seyfert 2's and 8 for composites, one obtains a starburst contribution to Hβ of 40% (precisely what we have derived above comparing composites and starburst galaxies in terms of $W_{\rm H\beta}^{\rm FC}$). Illustrative as these global estimates are, it is clear that both composite and "pure" systems present a *range* of properties. For the composites below NGC 5135 ([O III]/H$\beta = 4$) in Figures 10*c* and 10*d*, for instance, the same exercise would yield more than 70% of Hβ powered by the starburst. Much therefore remains to be learned from a more detailed object by object analysis.

4.4. *Emission Line Profiles: Kinematical Separation of the Starburst and AGN*

One prospect for disentangling the starburst and AGN contributions to the emission lines is to study their profiles in search of differential kinematical signatures of these two components. We have thus performed a line profile analysis for the Seyfert 2 sample, but only for the Kitt Peak data, which have higher spectral resolution.

Most of the composites have [O III] and Hβ profiles which can each be described in terms of two components. Interestingly, the narrower component often has a lower excitation than the broader one (Table 5), qualitatively consistent with them being powered by a starburst and an AGN, respectively. In fact, the excitation of the broad component (mean [O III]/H$\beta = 10.7$, standard deviation $= 2.8$) is very similar to the excitation of "pure" Seyfert 2's. However, the excitation of the narrow components ranges between 2.7 and 11.6. Meanwhile, the excitation in Mrk 1066, Mrk 1073, NGC 5135, NGC 7130, and IC 3639 is similar to the excitation in prototypical nuclear starbursts (e.g., NGC 7714, González-Delgado et al. 1995), while in Mrk 1, Mrk 463E, Mrk 477, and Mrk 533 the excitation is higher and similar to the excitation in young and very highly excited H II regions (e.g., NGC 2363, González-Delgado et al. 1994). The difference in excitation between these two subgroups within the composites is suggestive of evolutionary effects, where the youngest systems are the ones with highest excitation. This is consistent with other properties of composites, such as $W_{\rm H\beta}^{\rm FC}$, the fraction of total optical light provided by intermediate and young stars ($x_{\rm INT}/x_{\rm FC}$), and the detection of Wolf-Rayet features (see § 7.3).

If this interpretation is correct, i.e., the narrow and broad emission line components are produced by the starburst

TABLE 5

LINE PROFILE ANALYSIS OF COMPOSITES

Name	([O III]/Hβ)$_{\rm narrow}$	([O III]/Hβ)$_{\rm broad}$	$F_{\rm H\beta,narrow}/F_{\rm H\beta}$ (%)	$F_{\rm [OIII],narrow}/F_{\rm [OIII]}$ (%)
Mrk 1	11.6	11.5	38	38
Mrk 273	3.1[a]			
Mrk 463E	8.9	8.3	37	39
Mrk 477	8.8	8.7	58	59
Mrk 533	9.4	12.5	54	46
Mrk 1066	2.9	5.7	70	55
Mrk 1073	4.6	15.4	80	54
NGC 5135	2.7	10.5	80	54
NGC 7130	2.7	11.7	60	25
IC 3639	5.4	12.0	66	47

NOTES.—The principal properties of the two kinematic components fitted to the Hβ and [O III] λ5007 emission lines in the composites Seyfert 2 nuclei.

[a] The nuclear spectrum of Mrk 273 corresponds to the central 2.″1 × 1.″5 around the continuum maximum at 4450 Å. This maximum is shifted with respect to the maximum of the nebular emission lines. The [O III] map obtained by Colina, Arribas, & Borne 1999 shows an off-nucleus Seyfert 2 nebula 4″ south with a [O III]/H$\beta \sim 8$, similar to the excitation of the broad component in the other composites.

and AGN, respectively, the ratio of the narrow to total line flux gives an estimate of the starburst contribution to the ionization of the gas. For Hβ, this ratio ranges between 37% (in Mrk 463E) and 80% (in Mrk 1073 and NGC 5135), in agreement with our coarser estimates in § 4.3. These values suggest a significant impact of the circumnuclear starbursts upon the emission line ratios in Seyfert 2's.

4.5. *What Drives the Line-FC Correlations in Seyfert 2 Galaxies?*

The FC strength, $W^{\rm FC}$-values, emission line ratios, and profiles all consistently reflect the presence of circumnuclear starbursts in Seyfert 2's and can therefore be used as the empirical diagnostics of compositeness which we set out to identify in this paper. The line-FC correlations presented in Figures 7 and 8 do not play any direct part in such diagnostics. Nevertheless, because of their high statistical significance, potential relevance and controversial history, in this section we speculate on what might be driving them. We do this by contrasting two extreme views on the origin of the FC in "pure" Seyfert 2's.

4.5.1. *Starburst-Dominated FC*

Since we have established that circumnuclear starbursts make substantial contributions both to the FC and Hβ emission, and given that these two quantities are causally linked in starburst systems, *the presence of circumnuclear starbursts in Seyfert 2's naturally leads to a* Hβ-FC *correlation.* Even if the AGN components of $F_{\rm FC}$ and $F_{\rm H\beta}$ are uncorrelated, the starburst portions should suffice to maintain a Hβ-FC correlation in the combined AGN + starburst data.

One extreme interpretation of Figure 7*a* is thus that the Hβ-FC correlation is essentially driven by the presence of circumnuclear starbursts. If this is to apply to *all* sources, the FC must be dominated by the starburst *even in "pure" Seyfert 2's.* Varying proportions of starburst to AGN ionizing power can be invoked to account for the few "pure" Seyfert 2's whose Hβ/FC ratios exceed the maximum $W^{\rm FC}_{\rm H\beta} = 200$ Å reached by composites. This can be explained either by scaling up the nuclear ionizing source, thus increasing $F_{\rm H\beta}$ while keeping $F_{\rm FC}$ constant, or by scaling down the starburst, which also increases $W^{\rm FC}_{\rm H\beta}$ since $F_{\rm FC}$ would be more affected than $F_{\rm H\beta}$. Such adjustments can even be dispensed with if one allows for differential extinction to the line and FC, since we have seen in Figure 9*b* that this alone substantially reduces the $W^{\rm FC}_{\rm H\beta}$ differences between composite and "pure" systems.

But how do the [O III] (Fig. 8*a*) and He II-FC (Fig. 8*c*) correlations fit into this model? Table 4 shows that these correlations, while poorer than the one between $F_{\rm H\beta}$ and $F_{\rm FC}$, are still significant at the >99% confidence level and that the reason for the larger scatter is the small $W^{\rm FC}_{\rm [O\,III]}$ and $W^{\rm FC}_{\rm He\,II}$ of some five or six composites. Such a scatter is in fact expected in a starburst-dominated FC model, since the [O III] and (especially) the He II line fluxes trace the AGN power, whereas $F_{\rm FC}$ is a measure of the starburst power, so that $W^{\rm FC}_{\rm [O\,III]}$ and $W^{\rm FC}_{\rm He\,II}$ are indicators of the varying contrast between these components. Decreasing the power of the starbursts in composite systems by factors of 2–3 while keeping the AGN constant would move composites along roughly horizontal lines to the left in Figures 8*a* and 8*c*, placing them among "pure" Seyfert 2's.

While it is easy to see why composites deviate in $W^{\rm FC}_{\rm [O\,III]}$ and $W^{\rm FC}_{\rm He\,II}$, it is not clear why "pure" Seyfert 2's should define line-FC correlations as good as those revealed in Figures 7 and 8 (see also Table 4). If their FC is indeed dominated by a weak starburst, then the fact that their AGN-dominated $F_{\rm [O\,III]}$ and $F_{\rm He\,II}$ scale with $F_{\rm FC}$ would indirectly imply the existence of a *proportionality between the starburst and AGN powers*, i.e., that more powerful starbursts occur in more powerful AGNs! Further evidence for this scaling is presented in § 5, § 7.2, and GD01.

4.5.2. *AGN-Dominated FC*

An opposite model would be to postulate that the FC is dominated by starbursts *only* in composites, while in "pure" Seyfert 2's the FC is dominated by scattered light, so these two classes should not be mixed when discussing line-FC relations. This interpretation would lead us to the intriguing conclusion that the scattering efficiency, ϵ, which links the observed FC1 to the intrinsic nuclear FC via $L_{\rm FC1} = \epsilon L_{\rm FC0}$, does not vary substantially among Seyfert 2's. The surprise comes from the fact that ϵ depends on the geometry of the mirror and the optical depth of scattering particles (Miller, Goodrich, & Mathews 1991; Cid Fernandes & Terlevich 1995). Since there is no a priori reason why ϵ should be similar for all Seyfert 2's, we would expect a *wide spread* of $W^{\rm FC}$-values, contrary to the relatively narrow ranges observed, particularly if composites are excluded.

This argument has in fact been pursued by Mulchaey et al. (1994) to explain the *absence* of line-FC correlations in their data, from which they claim a consistency with the unified model. As acknowledged by Mulchaey et al., however, it is possible that, just as we find here, a substantial part of the scatter in their line-FC plots is associated with contamination by starburst activity. That this is more than a possibility is illustrated by the fact that the Seyfert 2 list of Mulchaey et al. (1994) includes 12 of our 15 composites! It also includes other prime composite suspects, most notably NGC 6221, a source for which Levenson et al. (2001a) find a complete dominance of the starburst, with the AGNs shining through only in hard X-rays. As a whole, their sample is similar to the NLAGN sample of SBMQ95 in terms of the mixed types of sources. Indeed, as seen in Figures 7*b*, 7*d*, and 8*b*, no line-FC correlations are present for this heterogeneous sample. Furthermore, contamination by starbursts is certainly larger in the Mulchaey et al. data than in ours, since they trace the FC by the far-UV flux collected through the large aperture of the *IUE* spectrometer, a procedure which follows the premise that starlight contamination is irrelevant in the UV. This premise was proven wrong by Heckman et al. (1995), who have demonstrated that, on the contrary, scattered light from a hidden Seyfert 1 is a minor contributor to the *IUE* spectra of Seyfert 2's, which are more typical of reddened starbursts.

At least in relative terms, it is clear that our observations are better suited to investigate line-FC relations. Our results essentially recover the classic Yee (1980) and Shuder (1981) correlation between line and FC luminosity, which extends over more than 5 decades in luminosity from Seyfert 2's to QSOs. Looking at their original plots one sees that Seyfert 2's show a larger scatter around the correlations than type 1 sources, but they still broadly follow the correlations. While it is true that the interpretation of their line-FC correlations was left orphan with the advent of the unified model, their reality has not been convincingly challenged as yet. Simi-

larly, barring unidentified selection effects, it is hard to deny the reality of the line-FC correlations seen in Figures 7 and 8.

In a $L_{FC} = L_{FC1}$ model $W_{H\beta}^{FC}$ equals $W_{H\beta}^{Sey1}\epsilon^{-1}$, where $W_{H\beta}^{Sey1}$ is the equivalent width which would be measured from nonobscured lines of sight to the Seyfert 1 nucleus. Observationally, the narrow Hβ in Seyfert 1's roughly spans the range between $W_{H\beta}^{Sey1} \sim 5$ to 75 Å (Goodrich 1989; Rodríguez-Ardila, Pastoriza, & Donzelli 2000). This spread is already comparable to the $70 \leq W_{H\beta}^{FC} \leq 560$ Å interval span by "pure" Seyfert 2's in our sample, which does not leave much room for a spread in ϵ. Combining these intervals we obtain an acceptable range for ϵ of roughly 0.01–0.1. (As a reference, for NGC 1068, the only source for which the scattering has been modeled in detail, $\epsilon \sim 0.015$; Miller et al. 1991). A "well behaved" ϵ is thus required in order to explain the Hβ-FC correlation for "pure" Seyfert 2's. This interpretation is analogous to, and just as puzzling as, the interpretation of the constancy of the W of broad Hβ among type 1 Seyferts and QSOs as due to a roughly constant covering fraction of broad line clouds in all sources (Yee 1980; Shuder 1981; Osterbrock 1989; Binette et al. 1993). While viable, this model obviously requires some fine tuning.

Yet another possibility is that the FC carries a sizable *nebular* component in "pure" Seyfert 2's, which would naturally produce line-FC correlations. A purely nebular FC, however, would produce $W_{H\beta}^{FC}$ of order 2000 Å for electron temperatures between 10,000 and 20,000 K, much larger than the values we find. A hotter plasma, however, can enhance the continuum emission and lower the W^{FC}-values. This is the essence of Tran's (1995c) model for FC2: emission from the $\sim 10^5$ K electron-scattering mirror. If this emission is somehow tied to the line emission—which is reasonable since both arise in circumnuclear gas heated by the active nucleus—then a line-FC correlation follows.

While our personal prejudices tend to favor a starburst-dominated FC interpretation, we are not in a position to rule out a role for a nonstellar FC for "pure" Seyfert 2's. Indeed, the fact that NGC 1068 mingles so well among composite starburst/Seyfert 2's is a clear demonstration that our analysis cannot resolve the ambiguous nature of the FC in "pure" Seyfert 2's. Since we know that several composites have a scattered component (Table 2), the correct interpretation of the line-FC relation will certainly involve a mixture of the extreme possibilities discussed above.

5. FAR-INFRARED LUMINOSITIES

In Figures 7–9 we have seen that, besides having smaller emission line W^{FC}-values, the tendency of composites to live preferentially among luminous sources allows them to be more clearly separated from "pure" Seyfert2's in line-FC diagrams. To evaluate this tendency in a reddening independent fashion, Figure 11*a* shows the far-IR luminosity, computed with the 60 and 100 μm *IRAS* bands (cf. Sanders & Mirabel 1996), against W_K for the Seyfert 2 sample. The tendency identified by GD01 for composites to be powerful IR emitters is clearly seen in this figure. Except for Mrk 1210, ESO 362-G8, and NGC 5643, all composites have $L_{FIR} > 10^{10}\ L_\odot$. The difference in median L_{FIR} between composites and "pure" Seyfert 2's is a factor of 5.

Comparison with Figure 11*b* shows that composites are also more powerful far-IR sources than typical Starburst galaxies, being more comparable to the merger systems

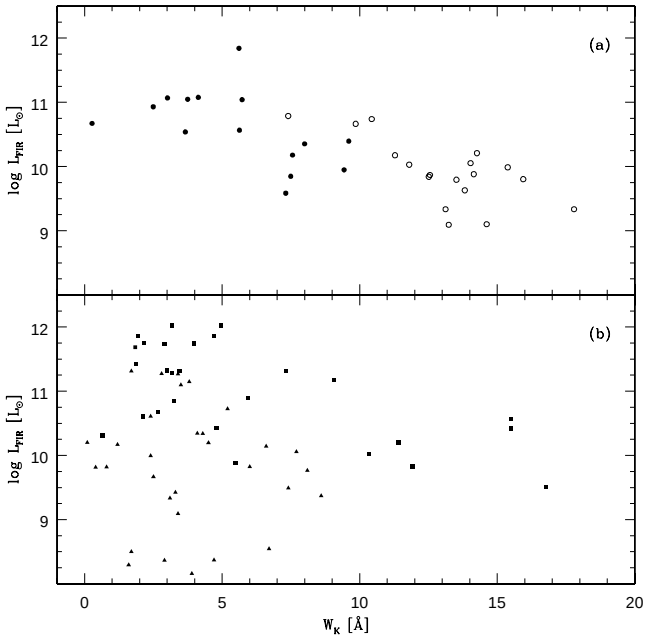

FIG. 11.—Far-IR luminosity against W_K for (*a*) the Seyfert 2 sample, and (*b*) the starburst and merger samples. Symbols as in Fig. 5. Starbursts with $L_{FIR} \leq$ few $\times 10^9\ L_\odot$ are generally blue compact dwarfs or related objects. Normal galaxies would populate the bottom part of the figure (i.e., low L_{FIR}), with W_K depending on the amount of star formation. Seyfert 2's lie along the upper envelope, with composites skewed to high L_{FIR}.

studied by LK95. Normal galaxies with little star formation would populate the large W_K and low L_{FIR} portion of the plot (Telesco 1988; Soifer, Houck, & Neugbauer 1987).

IR luminous galaxies have a well-known preference to be interacting systems (Sanders & Mirabel 1996). Figure 11*a* therefore suggests that interactions and the associated gas fueling of the nuclear regions may be a key ingredient in triggering circumnuclear starbursts in AGNs. Indeed, a substantial fraction of our composites (9 of 15) are associated with interacting systems or groups (GD01; Levenson et al. 2001b; SB00): NGC 7130, Mrk 1, Mrk 273, Mrk 463E, Mrk 477, Mrk 533, and IC 3639 are all in interacting systems, while NGC 5135 and NGC 7582 belong to groups. The analogous fraction for the "pure" Seyfert 2's is only 4 out of 20 (Mrk 348, Mrk 607, NGC 5929, and NGC 7212). This may explain why the composites resemble the mergers in Figure 11.

Since W_K works essentially as a measure of the starburst strength, Figure 11 indicates a link between the far-IR and the amount of recent star formation in Seyfert 2's. This link is investigated in Figure 12. The abscissa in Figure 12*a* is the total observed luminosity at 4861 Å, whereas in Figure 12*b* we filter out the light from old stars by using $L_{SB} \equiv L_{4861}^{obs} \times (x_{FC} + x_{INT})$. The poststarburst population, which was not included in the line-FC analysis because it does not ionize the gas, is now included because it can heat the dust. Furthermore, Table 4 shows that the far-IR flux is somewhat better correlated with F_{SB} than with F_{FC} alone. Comparison of Figures 12*a* and 12*b* show how $x_{FC} + x_{INT}$ has the property of unveiling a correlation immersed in the scatter when the whole continuum is used. An estimate of the effects of extinction is presented in Figure 12*c*, where we deredden L_{SB} using the Hα/Hβ values listed in Table 2. The bottom panels in Figure 12 show the corresponding results for Starburst galaxies and mergers. Comparison of the top

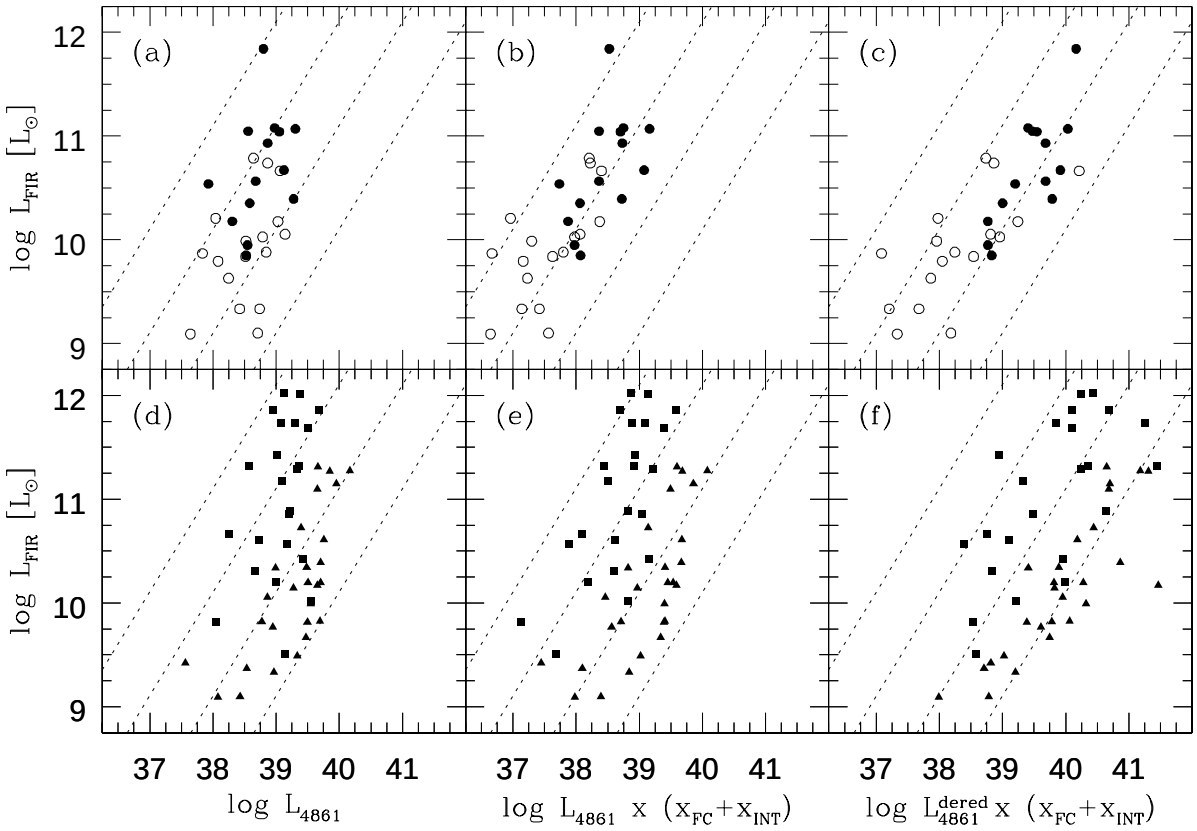

FIG. 12.—(*Top*) Relation between the far-IR and the continuum luminosity at 4861 Å for the Seyfert 2 sample. In (*a*) the total L_{4861} is used in the abscissa, whereas only the FC + poststarburst component is used in (*b*), and in (*c*) $L_{4861} \times (x_{FC} + x_{INT})$ is corrected for extinction (using Hα/Hβ). Composites are marked by filled circles. (*Bottom*) Same as above, but for the Starburst (*filled triangles*) and merger (*squares*) samples. Abscissa in units of ergs s^{-1} $Å^{-1}$. The dotted lines correspond to $L_{FIR}/(\nu L_\nu)_{4861}$ ratios of 1000, 100, 10, and 1.

and bottom panels shows that Seyfert 2's have F_{FIR}/F_{SB} ratios larger than galaxies in the Starburst sample, but compatible with the LK95 mergers. Despite the mixed emission line properties of the sources in the merger sample, it is reasonable to attribute most of their FIR and FC emission to star formation in a dusty environment (Lutz et al. 1998, 1999). This similarity is thus suggestive of the presence of powerful dusty circumnuclear starbursts in Seyfert 2's, consistent with our knowledge of composites. A usual caveat when dealing with *IRAS* fluxes is that one has to allow for the fact that a substantial fraction of the far-IR light originates well outside the nuclear region. Aperture effects may therefore be partially responsible for the larger F_{FIR}/F_{SB} found for objects in the Seyfert 2 than in the Starburst sample. This effect was detected for sources in common between the Seyfert 2 and NLAGN samples, the latter having systematically larger F_{SB} and thus smaller F_{FIR}/F_{SB}. At any rate, it is clear that circumnuclear starbursts can be responsible for the bulk of the far-IR emission in Seyfert 2's. This was in fact confirmed in the few cases where this issue has been examined more closely (e.g., Mrk 477 Heckman et al. 1997; see also Rigopoulou et al. 1999).

6. NEAR-ULTRAVIOLET SURFACE BRIGHTNESS

We have shown that the near-UV nuclear light in the Seyfert 2 composites is dominated by young and intermediate-age stars. In order to make some causal connection between these young stars and the Seyfert phenomenon, we must establish that the properties of this stellar population are unusual compared to the nuclei of normal galaxies. Young and intermediate-age stars dominate the near-UV continuum in the nuclei of normal galaxies of Hubble type Sbc and later (e.g., Heckman 1980). Seyfert galaxies are generally classified as early-type disk galaxies (e.g., Nelson & Whittle 1996; Ho, Filippenko, & Sargent 1997), whose nuclei are dominated by old stars. However, the Hubble types of Seyfert galaxies based on ground-based images are quite uncertain, since they are generally much more distant than the galaxies used to define the Hubble sequence. Indeed, the *HST* imaging survey by Malkan, Gorjian, & Tam (1998) reveals a significant number of Seyfert 2's (including some of our composites) in which the *HST*-based Hubble type is much later than that assigned from earlier ground-based images (Storchi-Bergmann et al. 2001). Could it be that the Seyfert 2 composites are simply otherwise normal late-type galaxies containing an AGN? The abnormally large far-IR luminosities of the composites argues against this. In this section we also show that the observed UV surface brightnesses of the Seyfert 2 composite nuclei are much larger than the nuclei of normal galaxies (of any Hubble type), but rather similar to typical starbursts.

We have compared the surface brightnesses in the near-UV ($\sim$3660 Å) of all our Seyfert 2's with those of normal galactic nuclei based on the imaging data published

by Jansen et al. (2000). For the normal nuclei (spanning the full range of Hubble types) we have computed the mean surface brightness through two metric apertures with radii of 250 and 500 pc, chosen to represent typical values of the spectroscopic apertures used for the Seyfert 2 nuclei (see Fig. 1). This was done converting the U-band surface photometry of Jansen et al. (2000) to monochromatic surface brightnesses at 3650 Å, including a correction for Galactic extinction (from NED). We have also measured near-UV surface brightnesses from the spectra of the starburst and merger samples. In these samples we have restricted our comparison to galaxies in which the projected aperture size of the spectra had a radius less than 1 kpc (see Fig. 1). Thus, in all cases we are comparing near-UV surface brightnesses on similar physical scales (radii of several hundred pc).

The results are shown in Figure 13, from which we draw the following conclusions. First, the Seyfert 2 composites have much higher central near-UV surface brightnesses than normal galaxies of any Hubble type (by roughly an order of magnitude on average). A correction for dust extinction would undoubtedly increase the disparity still further. Second, the Seyfert 2 composites have rather similar central near-UV surface brightnesses to the members of the Starburst and merger samples. When the near-UV surface brightness is corrected for extinction (see Fig. 14), the Seyfert 2 composites reach values similar to those which would be exhibited by the "maximal" starbursts studied by Meurer et al. (1997). Third, the Seyfert 2 composites have tend to have higher central near-UV surface brightness than the "pure" Seyfert 2's (by an average factor of about 2). As we show in Figure 14, the difference between the two classes is larger (factor of $\sim$4) when an extinction correction is made. Fourth, the "pure" Seyfert 2's overlap with the normal galactic nuclei having the highest UV surface brightnesses. These latter tend to be the nuclei of normal early-type (Sb and earlier) galaxies whose high UV surface brightness is due to their prominent bulge component. This is consistent with "pure" Seyfert 2's being otherwise normal early-type galaxies with only a modest contribution of light from an AGN or young stars (as shown by our spectral synthesis). Note that the outlying Seyfert 2 with extremely high surface brightness is the nucleus of NGC 1068 (due to the small physical size of the spectroscopic aperture and the strong contribution by scattered AGN light). Finally, Figure 14 also shows the expected trend between increasing UV surface brightness and an increasing relative contribution to the near-UV light by young and intermediate-age stars (as parameterized by W_K).

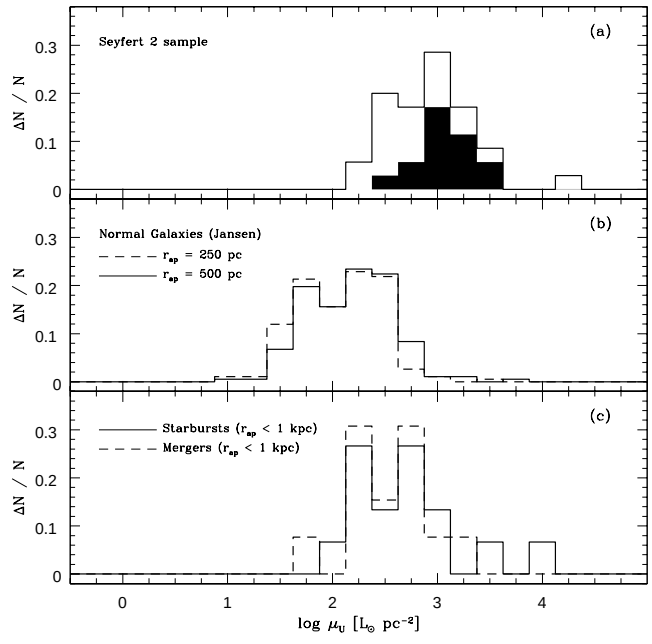

FIG. 13.—(*a*) Distribution of U-band surface brightness for the Seyfert 2 sample, with composites indicated by the filled areas. (*b*) As above, but for normal galaxies from the Jansen et al. (2000) catalog, extracted through 250 or 500 pc aperture radii. (*c*) As above but for the Starburst and merger samples, excluding sources observed through apertures larger than $r_{ap} = 1$ kpc. For the Seyfert 2, Starburst and merger samples μ_U was measured from the F_{3660} flux divided by the aperture area. For the Jansen et al. data μ_U comes from aperture photometry in U.

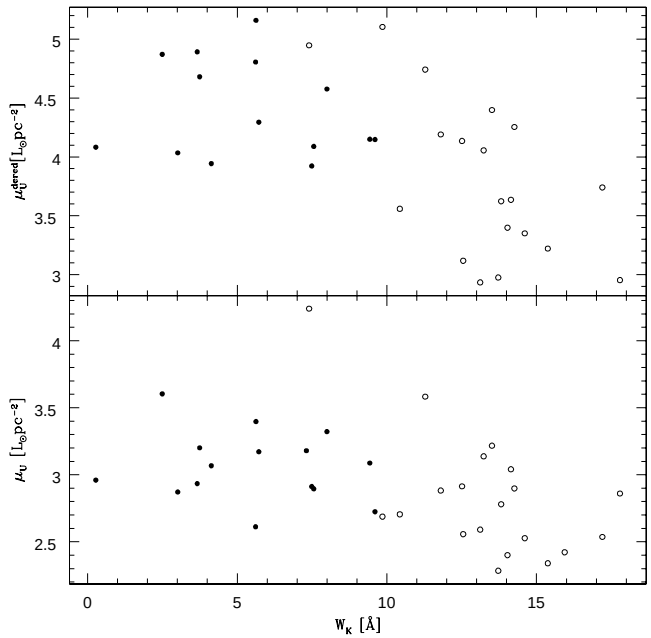

FIG. 14.—(*Bottom*) U-band surface brightness against W_K for the Seyfert 2 sample. (*Top*) Same as above after correcting μ_U by the extinction using Hα/Hβ. Considering that the extinction in the continuum can be smaller than that of the emission lines (Calzetti et al. 1994), panels (*a*) and (*b*) bracket the correct values for μ_U.

7. DISCUSSION

7.1. *Diagnostic of Compositeness*

Our experiments have consistently shown that Seyfert 2's with circumnuclear starbursts detected by means of either far-UV stellar wind lines, high-order Balmer absorption lines or the WR bump also present distinctive optical/near-UV continuum, optical emission line, far-IR continuum, and near-UV surface brightness properties, all in agreement with the expected impact of starbursts upon such observables. Given this remarkable consistency, one can use the results of our analysis as alternative tools to identify composite sources.

The following empirical criteria can be used to characterize a Seyfert 2 nucleus as composite:

1. Weak Ca II K: $W_K < 10$ Å. Or, equivalently, a small contribution of old stars: $x_{OLD} < 75\%$.

2. Weak emission lines with respect to the FC: $W^{FC}_{H\beta} < 200$ Å, $W^{FC}_{[O\,III]} < 2500$ Å, $W^{FC}_{[O\,II]} < 600$ Å.
3. Low excitation: He II/Hβ < 0.4, [O III]/Hβ < 15.
4. Large far-IR luminosity: $L_{FIR} \gtrsim 10^{10}\ L_\odot$.
5. Composite line profiles, with a narrow component typical of H II nuclei and a broader one with NLR-like excitation.
6. High near-UV surface brightnesses on circumnuclear scales: $\sim 10^3\ L_\odot\ pc^{-2}$ uncorrected for extinction and $\sim 10^4\ L_\odot\ pc^{-2}$ after extinction correction.

These criteria are laid roughly in order of importance, the Ca II K (or x_{OLD}) limit being by far the most useful. The upper limits for the W^{FC}-values and emission line ratios quoted above were chosen as to encompass all composites in our sample, most of which have substantially smaller values than those listed above. As argued above, one cannot base a classification on these properties alone, but they are useful to confirm the compositeness for sources satisfying the first criterion. Taken together, these empirical rules separate composite from "pure" systems very efficiently.

Naturally, there are borderline cases. The moderate FC ($15\% < x_{FC} < 30\%$) galaxies Mrk 3, Mrk 34, and NGC 7212, which we discussed in § 3.3.2, lie either within or close to the limits outlined above. The clearest distinction between these galaxies and our composites is in terms of their emission line W^{FC}-values, $W^{FC}_{H\beta} = 235$–321 and $W^{FC}_{[O\,III]} = 2667$–3565 Å, typical of "pure" Seyfert 2's but larger than in any of our composites, and well away from Starburst galaxies. Note, however, that these high W^{FC}-values, coupled with the dominant contribution of old stars ($x_{OLD} \sim 77\%$) are precisely the conditions under which the identification of starburst features are most difficult (§ 4.1.1), so we cannot rule out the possibility that their FC is dominated by relatively weak circumnuclear starbursts. The other moderate FC source in our sample is NGC 1068, for which there is overwhelming evidence that the nuclear optical FC is predominantly scattered AGN light. The similarities between this prototype Seyfert 2 and our composites, whose FC are dominated by starbursts, is a reminder of how similar starbursts and AGNs can be, and a demonstration of the limitations of our diagnostics for borderline cases.

Overall, the empirical criteria listed above fulfill our objective of delineating a region in a space of easily obtained observables which can be used to indirectly infer the presence of circumnuclear starbursts in Seyfert 2's. We therefore anticipate that their application to large samples of near-UV spectra will reveal many more composite systems. In fact, since these criteria mix several kinds of properties, it is not at all obvious whether they will hold for larger samples. Future applications of these diagnostics will therefore not only serve as a means of identifying composite candidates but to verify the consistency of the scheme as a whole. It will also be interesting to incorporate other multiwavelength data in order to help disentangling the starburst and AGN components. Valuable tools in this sense were developed for the IR part of the spectrum by Miley, Neugebauer, & Soifer (1985), Lutz et al. (1998), Genzel & Cesarsky (2000), Laurent et al. (2000), and Hill et al. (1999, 2001), among others. In the radio part of the spectrum, some of the diagnostics and techniques presented by Kewley et al. (2000), Smith et al. (1998a, 1998b), Lonsdale et al. (1993), and Condon et al. (1991) can be used, while X-ray signatures of circumnuclear starbursts have been recently investigated by Levenson et al. (2001b).

7.2. *A "Starburst $\propto$ AGN" Connection?*

We have shown that starburst/Seyfert 2 composites have large Hβ, FC, and far-IR luminosities within our sample. These are all quantities which may carry a significant, even dominant contribution from the starburst itself. In order to investigate whether these powerful starbursts are associated with correspondingly powerful AGNs we compared the [O III], He II, and 12 μm luminosities of composites and pure Seyfert 2's. These properties are less affected by the starburst component and thus provide an empirical measure of the AGN intensity.

We find that composites are also skewed toward large luminosities in all these properties. For instance, 53% of the sources above but just 31% of those below the median reddening-corrected $L_{[O\,III]}$ of 4.8×10^{41} ergs s^{-1} are composites. Nearly identical numbers apply to $L_{He\,II}$, while for $L_{12\mu m}$, which arguably measures the hot dust heated by the AGN (Pier & Krolik 1992; Spinoglio & Malkan 1989), the composite percentages are 65% and 25% above and below the median, respectively. These asymmetries are comparable to those in starburst-sensitive properties. For $L_{H\beta}$, for instance, we find 65% of composites above the median 6.0×10^{40} ergs s^{-1}, but just 19% below it. The corresponding numbers for L_{FIR} are 71% and 19%.

Circumnuclear starbursts in Seyfert 2's, at least those we can detect, are therefore powerful (bolometric luminosities of $\gtrsim 10^{10}\ L_\odot$, judging by L_{FIR}) and surround correspondingly powerful AGNs. This *luminosity link* between AGN and circumnuclear starburst activity can be interpreted in several ways. Perhaps the starburst activity stirs up the ISM in a way which induces a large rate of gas accretion by the central supermassive black hole (Colina & Wada 2000), while less powerful AGNs can be fed with more modest accretion rates, dispensing the helping hand of a circumnuclear starburst. While feasible, this does not seem to be the only mechanism to produce powerful AGNs, since there are also some high-luminosity "pure" Seyfert 2's in our sample. Or perhaps the "$L_{starburst} \propto L_{AGN}$" relation extends all over the L_{AGN} spectrum but is only detected for the most luminous AGNs because of our difficulties in identifying weak circumnuclear starbursts.

Whatever the correct interpretation, our results strongly suggest that powerful Seyfert 2's have at least a 1 in 2 chance of harboring detectable circumnuclear starbursts. This *prediction* can be readily tested by applying the diagnostics developed in this and our previous work to near-UV spectra of such systems, some of which have luminosities rivaling those of quasars (de Grijp et al. 1992). Extending the starburst-AGN connection studies toward the low-luminosity end, on the other hand, will require alternative techniques. High spatial resolution (i.e., *HST*) near-UV spectroscopy offers the best hope of maximizing the contribution of circumnuclear star-forming regions with respect to the old stellar population background. This technique was recently applied to the LINER NGC 3507 by Shields et al. (2000), where young stars previously undetected from the ground were clearly revealed with *HST*.

7.3. *The Meaning of Compositeness*

The composite versus "pure" Seyfert 2 classification which runs throughout this paper does not necessarily

reflect an intrinsic dichotomy among type 2 Seyferts. In the spirit of unification, one would rather prefer to look at these two classes as representing extremes of a continuous distribution of some underlying physical parameter. This view is warranted by the continuity and overlap in observed properties between composites and "pure" Seyfert 2's found in this and other studies (Levenson et al. 2001b; Veilleux 2001 and references therein).

At least two ingredients must be involved in any physical description of a starburst-AGN connection, one of which is some measure of the relative starburst to AGN intensities, such as the ratio of star formation to accretion rate, or the black hole to stellar mass ratio. Of the properties investigated in this paper the W^{FC}-values, mainly of [O III] and He II, and the excitation ratios [O III]/Hβ and He II/Hβ are in principle the ones more closely associated with this "starburst-to-AGN ratio." The fact that as a whole "pure" Seyfert 2's behave more like AGNs in terms of these indicators than composites is thus consistent with them having a smaller starburst-to-AGN ratio. The strongest contrast effect, however, is between the starburst and old stellar population, as deduced from the fact that *all* composites but only one "pure" Seyfert 2 have $x_{OLD} < 75\%$, a limit which can be expressed in a more empirical way by $W_K < 10$ Å. The Ca II K line originates in bulge stars, being neither a tracer of starburst nor AGN activity, so this threshold is clearly an observational limitation which prevents us from identifying circumnuclear starbursts not powerful enough to dilute W_K below 10 Å. The "pure" category ought to contain at least some such systems, and in fact several "pure" Seyfert 2's in our sample, particularly the less luminous ones (see Fig. 7), have W^{FC}-values and excitation ratios within the range spanned by composites.

The other ingredient is *evolution*. The combination of starburst-to-AGN ratios and evolution can in principle account for the whole range between composite and "pure" systems. While our coarse, three-component population synthesis analysis does not provide a detailed description of the evolutionary history of circumnuclear starbursts in Seyfert 2's, in § 3.2 we have seen that the relative strengths of x_{FC} and x_{INT} in composites bear a very good correspondence with the evolutionary status deduced from a much more detailed spectral analysis (SB00; GD01). The ratio x_{INT}/x_{FC} can thus be used as an empirical measure of the time elapsed since the onset of star formation, allowing us to broadly assess evolutionary trends in the data.

Figure 15 shows that younger systems have stronger Hβ, He II, and [O III] emission lines, which we tentatively interpret as evidence for evolutionary effects. Only composites are plotted, since only for them we can safely interpret the FC component as due to young stars and hence read x_{FC}/x_{INT} as an age indicator. Also, note that W-values in this figure are measured with respect to the whole "starburst flux" $F_{SB} = F_{obs}(x_{FC} + x_{INT})$. This choice of normalization facilitates the comparison with spectral evolution models such as Starburst99 (Leitherer et al. 1999), particularly for systems undergoing star formation over a period of order 10^8 yr. Since Hβ contains a strong contribution from gas ionized by the starburst, Figure 15*a* roughly traces the evolution of the starburst. The He II and [O III] to F_{SB} ratios, on the other hand, are measures of the relative power of the AGN and the starburst, and so Figure 15*b* and 15*c* can be used to assess the evolution of the AGN with respect to that of the starburst.

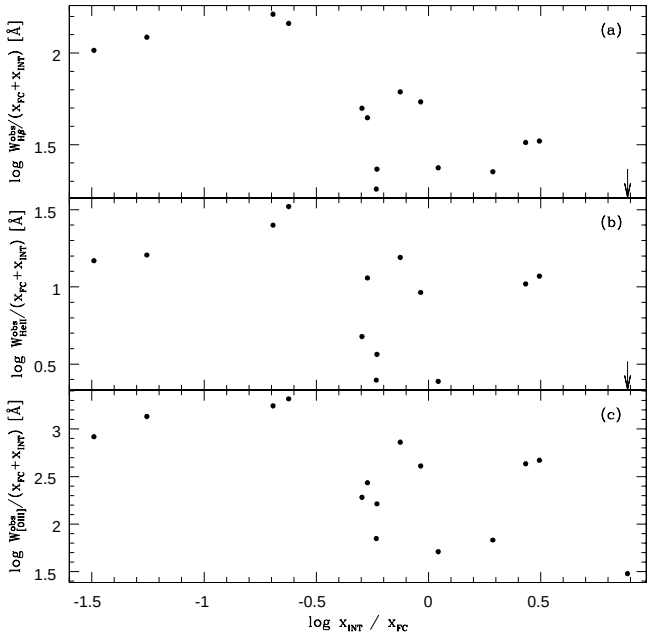

FIG. 15.—(*a*) "Evolution" of the Hβ equivalent width with respect to the continuum flux due to young and intermediate-age stars for the composites in the Seyfert 2 sample. The x_{INT}/x_{FC} axis is an empirical age indicator, which roughly maps onto a 0 to a few $\times 10^8$ yr age interval within the limits above. (*b*, *c*) As above, but for the AGN sensitive He II and [O III] lines. The arrow at the bottom right of (*a*) and (*b*) marks the horizontal position of ESO 362-G8, for which we did not measure Hβ nor He II emission.

As two extremes, we consider both an instantaneous burst and constant star formation to describe the starburst. In the former case, the optical continuum due to the young stars peaks in luminosity about 3 Myr after the burst and then fades by a factor of 3 by 10 Myr and by another factor of 10 by 50 Myr. The systematic decrease in $W_{He\,II}$ and $W_{[O\,III]}$ in the more evolved starbursts would therefore require that the AGN fades more rapidly than this. In this instantaneous burst scenario, the AGN lifetime must be very short in the composite Seyfert 2's ($<$ few $\times 10^7$ years). Since the AGNs should disappear before the intermediate-age stars, the descendants of the Seyfert 2 nuclei would be part of the poststarburst population (the "E + A" galaxies). Thus, the only plausible evolutionary link between the composite and "pure" Seyfert 2's would seemingly require that the latter are the evolutionary *precursors* to the former. This does not seem physically appealing because , among other reasons, the AGNs in the "pure" Seyfert 2's are significantly less powerful on-average than in their supposed descendants (the youngest composites). Moreover, an instantaneous burst description is clearly not appropriate for sources like NGC 5135 and NGC 7130, which contain a mix of young and intermediate-age stars.

Alternatively, we can consider a more long-lived ($\gg 10^7$ years) event in which the star formation remains roughly constant. The $W_{H\beta}$-values predicted by Starburst99 for constant star formation vary from 150–450 to 10–60 Å between 0 and 10^8 yr for different initial mass functions and solar metallicity. This range covers the values in Figure 15*a*. The $\sim$tenfold decrease in $W_{H\beta}$ during this period is also in agreement with the data. In this model, the luminosity of the optical continuum steadily grows with time (e.g., by a factor of 3 to 4 between 10 and 300 Myr after the start of the burst). The systematic decrease in $W_{He\,II}$ and $W_{O\,III}$ in the

more evolved starbursts would therefore imply that the AGNs luminosity remains relatively constant over this timescale. Long timescale bursts are indeed seen in pure starburst galaxies, where ground-based spectra usually integrate over regions containing several young, but noncoeval, superassociations (Meurer et al. 1995; González Delgado et al. 1998; Lançon et al. 2001). Individual starburst knots have been identified in some of our composites (González Delgado et al. 1998), so we expect this averaging effect to happen in Seyfert 2's too. In this scenario, both the starburst and AGN are relatively long-lived, and the AGN could well outlive the starburst. As the star formation ceases, the starburst will fade first in Hβ, then in the optical continuum, eventually reaching the point where only scattered FC and AGN-powered lines survive. With the drop in the starburst continuum the FC becomes weaker and W_K less diluted. Galaxies like ESO 362-G8, NGC 5643, and Mrk 78, with their weak FC but pronounced poststarburst populations, may represent this intermediate stage. [O III] and He II will be much less affected than Hβ by the death of massive stars, so excitation ratios will go up. Starburst-heated dust emission will subside, decreasing L_{FIR}. All these suggest that composites will end up as "pure" Seyfert 2's.

Clearly, the above is quite speculative. Eventually, it may be possible to test these ideas empirically with improved age dating techniques which will allow us to evolve detected starbursts back and forth in time and thus to evaluate whether the age of circumnuclear starbursts may be used as a clock for nuclear activity. As in any other astrophysical context where evolution is important, statistically significant samples will be necessary to trace all relevant stages.

8. CONCLUSIONS

We have examined a sample of 35 galaxies previously studied in a series of papers which addressed the occurrence of circumnuclear starbursts in Seyfert 2's and implications for the "starburst-AGN connection." The detailed spectral analysis performed in these previous papers was used to classify the nuclei into 15 composite and 20 "pure" Seyfert 2's, with composites defined as nuclei in which large populations of stars with ages of 10^6–10^8 yr have been conclusively detected either through UV stellar winds features, high-order Balmer absorption lines in the near-UV or the WR bump. Using this classification as a guide, we investigated continuum colors, absorption line equivalent widths, emission line properties, far-IR luminosities, and near-UV surface brightnesses for the sample galaxies and comparison samples of normal and Starburst galaxies, with the primary goal of verifying whether these properties reflect the presence of circumnuclear starbursts. Since this consistency was verified, these properties, all of which are more easily measured than those originally used to detect these starbursts, offer alternative empirical diagnostics of compositeness which can be applied to larger and more distant samples.

Our main results can be summarized as follows.

1. We have applied a semiempirical population synthesis method which effectively provides a biparametric description of each galaxy in terms of old ($\geq 10^9$ yr), poststarburst (10^8 yr) populations and a "featureless continuum" which represent the combined contribution of $\leq 10^7$ yr stars and a nonstellar FC. In practice, this representation requires little more than the equivalent width of the Ca II K line, and empirical calibrations were presented which allow an estimation of the (x_{OLD}, x_{INT}, x_{FC}) vector from W_K and the F_{3660}/F_{4020} color, both easy to measure observables. This very simple scheme proved instrumental in unveiling a number of properties and gives results which are consistent with a more detailed spectral analysis of the stellar population mixture.

2. *All* starburst/Seyfert 2 composites but *only one* "pure" Seyfert 2 (NGC 1068) have $x_{OLD} < 75\%$ at 4861 Å. This threshold can be expressed in a more empirical way by $W_K < 10$ Å. Given that our operational definition of composite/"pure" systems is based on the detection or otherwise of stellar features from massive stars, the most natural interpretation for this result is that it is due to a *contrast* effect: Seyfert 2's whose circumnuclear starbursts are overwhelmed by the light from the old stars in the host galaxy are not recognized as composite systems. At least some "pure" Seyfert 2's must fit this description, i.e., composites with weak starbursts. This may in fact apply to most, if not all, "pure" Seyfert 2's, since we cannot determine the nature of their weak UV excess with the data discussed here.

3. A related result is that strong FC sources, those with $x_{FC} \gtrsim 30\%$, are invariably associated with certified starburst/Seyfert 2 composites. We have argued that this is expected, since if scattered light was dominant in such sources then reflected broad lines would render them classified as type 1 Seyferts.

4. The equivalent widths of emission lines (Hβ, [O III], [O II]), when measured with respect to the FC, are larger in "pure" Seyfert 2's than in Starburst galaxies. Composites have W^{FC}-values intermediate between these two extremes. This fits with the idea that circumnuclear starbursts in Seyfert 2's contribute proportionately more to the FC than to the line flux, since, while the AGN-powered line emission is seen directly, only a small fraction of the corresponding nonstellar FC reaches the observer after scattering.

5. Part of the separation in $W^{FC}_{H\beta}$ between "pure" Seyfert 2's and composites may be due to another contrast effect, in which the high-order Balmer lines, the main diagnostic of massive stars in the optical, are diluted and eventually filled by nebular emission in strong lined sources, preventing them from being recognized as composites.

6. Composite systems tend to be less excited in terms of the He II/Hβ and [O III]/Hβ ratios. This indicates that the circumnuclear starbursts have a direct impact on the emission line properties of Seyfert 2's, with typically $\sim 50\%$ of Hβ being powered by OB stars.

7. The dual nature of the ionizing source in composites also leaves a kinematical imprint on the emission line profiles, which can be described in terms of a broad component with NLR-like line ratios and a narrower and (usually) less excited one. These components are presumably associated with the gas ionized by the AGN and starburst, respectively.

8. Composite galaxies are luminous in the far-IR, with $L_{FIR} \sim 10^{10}$ to 10^{12} $L_\odot$, and are more luminous than "pure" Seyfert 2's and normal galaxies. As a whole, composites are rather similar to merger systems in terms of their far-IR properties. About 50% of the composites, but only 20% of "pure" Seyfert 2's are in interacting systems, suggesting that galaxy interactions spur circumnuclear starbursts.

9. Composite galaxies have near-UV surface brightnesses in their centralmost few hundred parsecs that are on

average an order of magnitude higher than in normal galaxies of any Hubble type. These high surface brightnesses are similar to those in pure Starburst galaxies. They are also several times higher on average than in the "pure" Seyfert 2's (whose central surface brightnesses in most cases overlap those of normal early-type galaxies).

10. These properties were condensed into a set of empirical criteria which separate composite from "pure" systems. Most of the diagnostic power resides in the $W_K < 10$ Å limit. Other properties (small emission line W^{FC}, low excitation, and large L_{FIR}) serve to confirm the W_K-based diagnostic of compositeness and to judge borderline cases. We predict that many more starburst/Seyfert 2 composites will be uncovered by applying these diagnostics to large samples of near-UV spectra.

11. The tendency of composites with older starbursts to have smaller Hβ, He II, and [O III] emission line equivalent widths was tentatively interpreted as a sign of the evolution of circumnuclear starbursts in Seyfert 2's. Circumnuclear starbursts which are powerful today may fade away and, barring evolution of the active nucleus, appear as "pure" Seyfert 2's. By improving the dating techniques and enlarging the databases we hope to trace this evolutionary sequence and thereby put strong constraints on physical scenarios for the starburst-AGN connection.

It is a pleasure to thank the organizers and participants of the Guilllermo Haro 2000 INAOE workshop on "The Starburst-AGN Connection," for a stimulating meeting in which this work was conceived. We would like to thank R. A. Jansen and C. T. Liu for making their data available. R. C. F. thanks the hospitality of Johns Hopkins University, where this work was developed, and the support provided by the National Science Foundation through grant GF-1001-99 from the Association of Universities for Research in Astronomy, Inc., under NSF cooperative agreement AST96-13615. Partial support from CNPq and PRONEX are also acknowledged. HRS work was supported by NASA under grant NAG5-9343. The National Radio Astronomy Observatory is a facility of the National Science Foundation operated under cooperative agreement by Associated Universities, Inc.

REFERENCES

Alonso-Herrero, A., Ward, M. J., Aragon-Salamanca, A., & Zamorano, J. 1999, MNRAS, 302, 561
Antonucci, R. R. J., & Miller, J. S. 1985, ApJ, 297, 621
Aretxaga, I., Joguet, B., Kunth, D., & Melnick, J., & Terlevich, R. J. 1999, ApJ, 519, L123
Aretxaga, I., Kunth, D., & Mugica, R. 2001, The Starburst-AGN Connection (Singapore: World Scientific)
Bassani, L., Dadina, M., Maiolino, R., Salvati, M., Risaliti, G., della Ceca, R., Matt, G., & Zamorani, G. 1999, ApJS, 121, 473
Bica, E. 1988, A&A, 195, 76
Binette, L., Fosbury, R. A., & Parker, D. 1993, PASP, 105, 1150
Boisson, C., Joly, M., Moultaka, J., Pelat, D., & Serote Roos, M. 2000, A&A, 357, 850
Byrd, G. G., Valtonen, M. J., Sundelius, B., & Valtaoja, L. 1986, A&A, 166, 75
Byrd, G. G., Sundelius, B., & Valtonen, M. J. 1987, A&A, 171, 16
Caganoff, S., et al. 1991, ApJ, 377, L9
Calzetti, D., Kinney, A., & Storchi Bergmann, T. 1994, ApJ, 429, 582
Cardeli, J. A., Clayton, G. C., & Mathis, J. S. 1989, ApJ, 345, 245
Cid Fernandes, R., Sodré, L., Schmitt, H., & Leão, J. R. 2001, MNRAS, 325, 60
Cid Fernandes, R. J., Storchi-Bergmann, T., & Schmitt, H. R. 1998, MNRAS, 297, 579
Cid Fernandes, R. J., & Terlevich, R. 1995, MNRAS, 272, 423
Colina, L., Arribas, S., & Borne, K. D. 1999, ApJ, 527, L13
Colina, L., Vargas, M. L. G., Delgado, R. M. G., Mas-Hesse, J. M., Perez, E., Alberdi, A., & Krabbe, A. 1997, ApJ, 488, L71
Colina, L., & Wada, K. 2000, ApJ, 529, 845
Condon, J. J., Huang, Z.-P., Yin, Q. F., & Thuan, T. X. 1991, ApJ, 378, 65
Dahari, O., & de Robertis, M. M. 1988, ApJS, 67, 249
Daly, R. A. 1990, ApJ, 355, 416
de Grijp, M. H. K., Keel, W. C., Miley, G. K., Goudfrooij, P., & Lub, J. 1992, A&AS, 96, 389
Ferrarese, L., & Merritt, D. 2000, ApJ, 539, L9
Fosbury, R. A. E., Vernet, J., Villar-Martín, M., Cohen, M. H., Ogle, P. M., & Tran, H. D. 1999, in The Most Distant Radio Galaxies, ed. H. J. A. Röttgering, P. N. Best, & M. D. Lehnert (Amsterdam: Royal Netherlands Acad.), 311
Gallagher, J. S., Bushouse, H., & Hunter, D. A. 1989, AJ, 97, 700
Gebhardt, K., et al. 2000, ApJ, 539, L13
Genzel, R., & Cesarsk, C. J. 2000, ARA&A, 38, 761
Gonçalves, A., Véron-Cetty, M.-P., Véron, P. 1999, A&AS, 135, 437
Gonzalez-Delgado, R. M., et al. 1994, ApJ, 437, 239
Gonzalez-Delgado, R. M., Perez, E., Diaz, A. I., Garcia-Vargas, M. L., Terlevich, E., & Vilchez, J. M. 1995, ApJ, 439, 604
González Delgado, R. M., Heckman, T., Leitherer, C., Meurer, G., Krolik, J., Wilson, A. S., Kinney, A., & Koratkar, A. 1998, ApJ, 505, 174
González Delgado, R. M., Heckman, T., & Leitherer, C. 2001, ApJ, 546, 845 (GD01)
Goodrich, R. W. 1989, ApJ, 342, 224
Goodrich, R. W., & Miller, J. S. 1989, ApJ, 346, L21
Heckman, T. M. 1980, A&A, 87, 142
Heckman, T., et al. 1995, ApJ, 452, 549
Heckman, T. M., Gonzalez-Delgado, R., Leitherer, C., Meurer, G. R., Krolik, J., Wilson, A. S., Koratkar, A., & Kinney, A. 1997, ApJ, 482, 114
Heisler, C. A., Lumsden, S. L., & Bailey, J. A. 1997, Nature, 385, 700
Heller, C. H., & Shlosman, I. 1994, ApJ, 424, 84
Hernquist, L., & Mihos, J. C. 1995, ApJ, 448, 41
Hill, T. L., Heisler, C. A., Norris, R. P., Reynolds, J. E., & Hunstead, R. W. 2001, AJ, 121, 128
Hill, T. L., Heisler, C. A., Sutherland, R., & Hunstead, R. W. 1999, AJ, 117, 111
Ho, L. 1999, in Observational Evidence for Black Holes in the Universe, ed. S. K. Chakrabarti (Dordrecht: Kluwer), 157
Ho, L. C. Filippenko, A. V., & Sargent, W. L. W. 1997, ApJ, 487, 568
Jansen, R. A., Franx, M., & Fabricant, D. 2001, ApJ, 551, 825
Jansen, R. A., Franx, M., Fabricant, D., & Caldwell, N. 2000, ApJS, 126, 271
Kay, L. E. 1994, ApJ, 430, 196
Keel, W. C. 1996, PASP, 108, 917
Kennicutt, R. C., Jr. 1992, ApJ, 388, 310
———. 1998, ARA&A, 36, 189
Kewley, L. J., Heisler, C. A., Dopita, M. A., Sutherland, R., Norris, R. P., Reynolds, J., & Lumsden, S. 2000, ApJ, 530, 704
Koski, A. T. 1978, ApJ, 223, 56
Kotilainen, J. K., & Ward, M. J. 1997, A&AS, 121, 77
Lançon, A., Goldader, J. D., Leitherer, C., & González Delgado, R. M. 2001, ApJ, 552, 150
Laurent, O., Mirabel, I. F., Charmandaris, V., Gallais, P., Madden, S. C., Sauvage, M., Vigroux, L., & Cesarsky, C. 2000, A&A, 359, 887
Leitherer, C. 1999, in ASP Conf. 192, Spectrophotometric Dating of Stars and Galaxies, ed. I. Hubeny, S. Heap, & R. Cornett (San Francisco: ASP), 3
Leitherer, C., et al. 1999, ApJS, 123, 3
Lester, D. F., Joy, M., Harvey, P. M., Ellis, H. B., & Parmar, P. S. 1987, ApJ, 321, 755
Levenson, N., Cid Fernandes, R., Weaver, K., Heckman, T., & Storchi-Bergmann, T. 2001a, ApJ, in press (astro-ph/0104316)
Levenson, N., Heckman, T., Weaver, K. 2001b, ApJ, 550, 230
Lin, D. N. C., Pringle, J. E., & Rees, M. J. 1988, ApJ, 328, 103
Liu, C. T., & Kennicutt, R. C. 1995a, ApJ, 450, 547 (LK95)
———. 1995b, ApJS, 100, 325 (LK95)
Lonsdale, C. J., Smith, H. E., & Lonsdale, C. J. 1993, ApJ, 405, L9
Lutz, D., Spoon, H. W. W., Rigopoulou, D., Moorwood, A. F. M., & Genzel, R. 1998, ApJ, 505, L103
Lutz, D., Veilleux, S., & Genzel, R. 1999, ApJ, 517, L13
Magorrian, J., et al. 1998, AJ, 115, 2285
Malkan, M. A., & Filippenko, A. V. 1983, ApJ, 275, 477
Malkan, M. A., Gorjian, V., & Tam, R. 1998, ApJS, 117, 25
Maoz, D., Koratkar, A., Shields, J. C., Ho, L. C., Filippenko, A. V., & Sternberg, A. 1998, AJ, 116, 55
McQuade, K., Calzetti, D., & Kinney, A. L. 1995, ApJS, 97, 331 (SBMQ95)
Merrifield, M. R., Forbes, D. A., & Terlevich, A. 2000, MNRAS, 313, L29
Meurer, G. R., Heckman, T. M., Lehnert, M. D., Leitherer, C., & Lowenthal, J. 1997, AJ, 114, 54
Meurer, G. R., Heckman, T. M., Leitherer, C., Kinney, A. L., Robert, C., & Garnett, D. R. 1995, AJ, 110, 2665
Mihos, J. C., & Hernquist, L. 1996, ApJ, 464, 641
Miley, G. K., Neugebauer, G., & Soifer, B. T. 1985, ApJ, 293, L11
Miller, J. S., & Antonucci, R. R. J. 1983, ApJ, 271, L7
Miller, J. S., & Goodrich, R. W. 1990, ApJ, 355, 456
Miller, J. S., Goodrich, R. W., & Mathews, W. G. 1991, ApJ, 378, 47

Moran, E. C., Barth, A. J., Kay, L. E., & Filippenko, A. V. 2000, ApJ, 540, L73
Mulchaey, J. S., Koratkar, A., Ward, M. J., Wilson, A. S., Whittle, M., Antonucci, R. R. J., Kinney, A. L., & Hurt, T. 1994, ApJ, 436, 586
Nelson, C., & Whittle, M. 1996, ApJ, 465, 96
Norman, C., & Scoville, N. 1988, ApJ, 332, 124
Norris, R. P., Allen, D. A., Sramek, R. A., Kesteven, M. J., & Troup, E. R. 1990, ApJ, 359, 291
Oliva, E., Origlia, L., Kotilainen, J. K., & Moorwood, A. F. M. 1995, A&A, 301, 55
Oliva, E., Origlia, L., Maiolino, R., & Moorwood, A. F. M. 1999, A&A, 350, 9
Ogle, P. M., Cohen, M. H., Miller, J. S., Tran, H. D., Fosbury, R. A. E., & Goodrich, R. W. 1997, ApJ, 482, L37
Osterbrock, D. E. 1983, PASP, 95, 12
———. 1989, Astrophysics of Gaseous Nebulae and Active Galactic Nuclei (Mill Valley: University Science Books)
Perry, J. J., & Dyson, J. E. 1985, MNRAS, 213, 665
Pier, E. A., & Krolik, J. H. 1992, ApJ, 401, 99
Pogge, R. W. 1989, ApJS, 71, 433
Pogge, R. W., & de Robertis, M. M. 1993, ApJ, 404, 563
Rees, M. J. 1989, MNRAS, 239, 1
Rigopoulou, D., Spoon, H. W. W., Genzel, R., Lutz, D., Moorwood, A. F. M., & Tran, Q. D. 1999, AJ, 118, 2625
Rodrigues-Lacerda, R. 2001, M.Sc. thesis, Univ. Federal de Santa Catarina
Rodríguez-Ardila, A., Pastoriza, M. G., & Donzelli, C. J. 2000, ApJS, 126, 63
Sanders, D. B., & Mirabel, I. F. 1996, ARA&A, 34, 749
Sanders, D. B., Soifer, B. T., Elias, J. H., Madore, B. F., Matthews, K., Neugebauer, G., & Scoville, N. Z. 1988, ApJ, 325, 74
Schaerer, D. 2001, in Starbursts—Near and Far, ed. L. Tacconi-Garman, D. Lutz (Berlin: Springer), in press (astro-ph/0012403)
Schlegel, D. J., Finkbeiner, D. P., & Davis, M. 1998, ApJ, 500, 525
Schmidt, A. A., Copetti, M. V. F., Alloin, D., & Jablonka, P. 1991, MNRAS, 249, 766
Schmitt, H. 1998, Ph.D. thesis, Insituto de Física, Univ. Federal do Rio Grande do Sul
Schmitt, H. R., Storchi-Bergmann, T., & Cid Fernandes, R. C. 1999, MNRAS, 303, 173
Shields, J. C., Sabra, B. M., Ho, L. C., Barth, A. J., & Filippenko, A. V. 2000, AAS, 197, 110.04
Shuder, J. M. 1981, ApJ, 244, 12
Smith, H. E., Lonsdale, C. J., & Lonsdale, C. J. 1998a, ApJ, 492, 137
Smith, H. E., Lonsdale, C. J., Lonsdale, C. J., & Diamond, P. J. 1998b, ApJ, 493, L17
Sodré, L., & Cuevas, H. 1997, MNRAS, 287, 137
Soifer, B. T., Houck, J. R., & Neuguebauer, G. 1987, ARA&A, 25, 187
Spinoglio, L., & Malkan, M. A. 1989, ApJ, 342, 83
Sramek, R. A., & Weedman, D. W. 1986, ApJ, 302, 640
Storchi-Bergmann, T., Bica, E., Raimann, D., & Fraquelli, H. 2000, ApJ, 544, 747 (SB00)
Storchi-Bergmann, T., Cid Fernandes, R. C., & Schmitt, H. R. 1998, ApJ, 501, 94
Storchi-Bergmann, T., González Delgado, R., Schmitt, H. R., Heckman, T., & Cid Fernandes, R. C. 2001, ApJ, in press (astro-ph/0105538)
Storchi-Bergmann, T., Kinney, A. L., & Challis, P. 1995, ApJS, 98, 103 (SBMQ95)
Storchi-Bergmann, T., Wilson, A. S., & Baldwin, J. A. 1996, ApJ, 460, 252
Tadhunter, C. N., Scarrott, S. M., & Rolph, C. D. 1990, MNRAS, 246, 163
Telesco, C. M. 1988, ARA&A, 26, 343
Telesco, C. M., Becklin, E. E., Wynn-Williams, C. G., & Harper, D. A. 1984, ApJ, 282, 427
Terlevich, E., Diaz, A. I., & Terlevich, R. 1990, MNRAS, 242, 271
Terlevich, R., Melnick, J., Masegosa, J., Moles, M., & Copetti, M. V. F. 1991, A&AS, 91, 285
Terlevich, R., Tenorio-Tagle, G., Franco, J., & Melnick, J. 1992, MNRAS, 255, 713
Tran, H. D. 1995a, ApJ, 440, 565
———. 1995b, ApJ, 440, 578
———. 1995c, ApJ, 440, 597
Tresse, L., Maddox, S., Loveday, J., & Singleton, C. 1999, MNRAS, 310, 262
Veilleux, S. 2001, in Starbursts—Near and Far, ed. L. Tacconi-Garman & D. Lutz (Berlin: Springer), in press
Véron, P., Goncalves, A. C., & Véron-Cetty, M. -. 1997, A&A, 319, 52
Viegas-Aldrovandi, S. M. 1988, ApJ, 330, L9
Wang, J., Heckman, T. M., Weaver, K. A., & Armus, L. 1997, ApJ, 474, 659
Williams, R. J. R., Baker, A. C., & Perry, J. J. 1999, MNRAS, 310, 913
Wilson, A. S., Helfer, T. T., Haniff, C. A., & Ward, M. J. 1991, ApJ, 381, 79
Wilson, A. S., Shopbell, P. L., Simpson, C., Storchi-Bergmann, T., Barbosa, F. K. B., & Ward, M. J. 2000, AJ, 120, 1325
Yee, H. K. C. 1980, ApJ, 241, 894